

Impact of Charge on Complexity Analysis and Isotropic Decoupled Solutions in $f(\mathbb{R}, \mathbb{T})$ Gravity

M. Sharif¹ * and Tayyab Naseer^{1,2} †

¹ Department of Mathematics and Statistics, The University of Lahore, 1-KM Defence Road Lahore-54000, Pakistan.

² Department of Mathematics, University of the Punjab, Quaid-i-Azam Campus, Lahore-54590, Pakistan.

Abstract

In this paper, we formulate two exact charged solutions to the field equations by extending the domain of existing anisotropic models with the help of minimal gravitational decoupling in $f(\mathbb{R}, \mathbb{T})$ theory. For this, the anisotropic fluid distribution is considered as a seed source that is extended through the inclusion of a new gravitational source. The influence of the later matter configuration is controlled by the decoupling parameter. We formulate the field equations corresponding to the total matter source that are then decoupled into two distinct sets by implementing a transformation only on the radial metric coefficient. Both of these under-determined sets correspond to their parent sources. Some well-behaved forms of the metric potentials are taken into account to deal with the first set of equations. On the other hand, we solve the second set corresponding to an additional source by taking different constraints on the matter sector. We then consider the radius and mass of a compact star $4U\ 1820-30$ to analyze the physical feasibility of the resulting solutions for a particular modified model. It is concluded that our resulting solutions show stable behavior for certain values of the decoupling parameter and charge.

*msharif.math@pu.edu.pk

†tayyabnaseer48@yahoo.com

Keywords: $f(\mathbb{R}, \mathbb{T})$ theory; Anisotropy; Self-gravitating systems; Gravitational decoupling.

PACS: 04.50.Kd; 04.40.Dg; 04.40.-b.

1 Introduction

Cosmological breakthroughs show that astrophysical structures are not scattered randomly in our cosmos but are systematically distributed. The analysis of such an integrated paradigm as well as different physical characteristics of compact self-gravitating objects enable astronomers to expose the accelerated expansion of the universe. Multiple modifications to general relativity (\mathbb{GR}) have been suggested to explain such a cosmic expansion in the recent couple of years. The insertion of the generic function of the Ricci scalar in place of \mathbb{R} in the Einstein-Hilbert action produces the first and straightforward extension of \mathbb{GR} , termed the $f(\mathbb{R})$ theory. Several researchers made an initial attempt to explain different evolutionary eras of the universe by adopting modified $f(\mathbb{R})$ models [1, 2]. The stability of this theory has also been addressed through different techniques [3, 4].

Bertolami et al. [5] initially merged the geometric terms with the matter Lagrangian density in $f(\mathbb{R})$ framework to produce the effects of fluid-geometry coupling on the test particles of massive bodies. Several researchers studied such coupling and concluded that it would be advantageous to discuss the cosmic accelerated expansion in this framework. Harko et al. [6] generalized this interaction by introducing a generic function of \mathbb{R} and trace of the energy-momentum tensor (\mathbb{EMT}) \mathbb{T} in the action, referred the $f(\mathbb{R}, \mathbb{T})$ theory. The coupling between geometry and matter in this framework provides non-vanishing divergence of the \mathbb{EMT} . An extra force thus appears in the gravitational field that changes the geodesic motion of the particles under consideration. Different gravitational aspects have been comprised by this theory due to the entanglement of the entity \mathbb{T} . Houndjo [7] considered a minimal model of this gravity and explained the transformation of the matter-dominated phase into late-time acceleration era. Das et al. [8] adopted the $\mathbb{R} + 2\chi_3\mathbb{T}$ model to explore the structure of gravastar comprising three different layers which are expressed by their respective equations of state. Different matter distributions have been discussed for such modified models from which various acceptable solutions representing compact interiors are obtained [9]-[15].

It is worth noting that the problem of the cosmological constant (Λ) can considerably be resolved through a particular choice such as $\mathbb{R} + 2\chi_3\mathbb{T}$. It has been shown that the constant Λ can be expressed in proportional relation with the Hubble parameter ($\mathbb{H} = \frac{\dot{\mathbf{a}}}{\mathbf{a}}$, where \mathbf{a} denotes the scale factor of the cosmos), i.e., $\Lambda_{eff} \propto \mathbb{H}^2$ [16]. The second term in the above model is a valid one that could generate several new insights and helps to understand the astronomical structures in a proper way [17, 18]. The model parameter has been restricted as $\chi_3 > -3.0 \times 10^{-4}$ while studying massive white dwarfs [19]. In addition, the background evolution provided a limit on this parameter as $-0.1 < \chi_3 < 1.5$ [20]. Also, the lower bound of χ_3 was obtained as -1.9×10^{-8} from the dark energy density parameter [21]. Ashmita et al. [22] adopted three different inflation potentials in this modified theory, and derived the corresponding field equations and potential slow-roll parameters. They concluded that their results are compatible with the observational data only for $-0.37 < \chi_3 < 1.483$. Kaur et al. [23] assumed this model to discuss the interior of charged anisotropic Tolman-Kuchowicz solution and found it stable as well as viable.

The nature of compact stellar bodies in our universe can be understood by formulating the solutions (exact or numerical) of their respective field equations. The highly non-linear nature of such equations prompted several astrophysicists to find different techniques so that these equations can be solved easily which further helps to check the physical relevancy of the respective model. One of the multiple approaches discussed in the literature is the gravitational decoupling that helps to obtain the feasible solution of the interior fluid distribution possessing multiple factors like pressure anisotropy, heat dissipation and shear stress. This approach solves the field equations corresponding to more than one matter configuration by transforming the metric components to a new frame of reference which makes much easier to solve them. Gravitational decoupling offers two schemes, one of them is the minimal geometric deformation (MGD). Ovalle [24] recently developed this approach and found the analytic solutions representing stellar objects in the braneworld (BW). Later, Ovalle and Linares [25] formulated an exact solution to the field equations for an isotropic sphere by using the MGD technique along with the Tolman-IV metric potentials in the BW scenario. Casadio et al. [26] developed a consistent extension of the above technique and proposed a new solution in the context of BW that helps to discuss the geometry of stars.

Ovalle et al. [27] employed the gravitational decoupling through MGD

approach and extended an isotropic solution to the anisotropic domain. They also analyzed the feasibility of resulting solutions through graphical interpretation. These isotropic solutions were then extended to the case of charged Krori-Barua anisotropic sphere in which the influence of an electromagnetic field on the stability of resulting models has been checked [28]. Gabbanelli et al. [29] developed the anisotropic Duragpal-Fuloria models representing physically relevant celestial objects. The same analysis has also been done for multiple extensions of the isotropic Heintzmann as well as Tolman VII spacetimes [30, 31]. The MGD approach was also used to extend several isotropic spacetimes to an acceptable anisotropic domain in Brans-Dicke theory [32]. Multiple compact models have been developed in a non-minimal gravitational theory through the decoupling technique [33]. The influence of the respective parameter was also checked on the corresponding physical determinants.

The analysis of self-gravitating celestial systems has been observed to be significantly affected by the presence of an electric charge. A strongly attractive nature of gravity can be reduced or counterbalanced through some important ingredients, one of them is the electromagnetic force. For this reason, a compact body needs a sufficient amount of the charge in order to resist the gravitational attraction and preserve its stable state. This has been confirmed by Bekenstein [34] while studying a charged dynamical sphere. He concluded that the nature of the electromagnetic force is opposite to that of gravity, helping the considered geometry to be stable. Esculpi and Aloma [35] have extended this work to explore the behavior of anisotropic matter distribution in a compact interior. They observed that the spacetime experiences a repulsive force due to the presence of both charge and positive anisotropy. Some anisotropic charged compact stars have been studied by adopting a particular form of the interior charge in terms of the spherical radius and acceptable results were obtained [36, 37]. Pretel et al. [38] explored the interior distribution of charged quark stars through a linear equation of state in the context of $\mathbb{R} + 2\chi_3\mathbb{T}$ gravity. They observed that the parameters measuring the impact of charge and modified theory considerably affect the total mass and radius of the star. Several physically relevant charged compact stars have been modeled by us in a non-minimally coupled framework [39].

Herrera [40] suggested a very recent definition of the complexity for static self-gravitation spherical systems. He used Bel's idea for the orthogonal decomposition of the curvature tensor corresponding to the anisotropic matter configuration and found several scalars. It was then observed that there

is only one scalar that involves the inhomogeneous density and anisotropy, thus referred as the complexity factor. This definition becomes widely accepted for the last couple of years in the scientific community. Herrera with his collaborators also extended this definition for dynamical matter source [41]. Such extensions have been developed in non-minimally coupled theory for static/non-static spherical and cylindrical interiors [42, 43]. Different constraints have been used in the literature to make the system solvable. Several researchers [44] used the complexity-free condition as a constraint and merged it with the decoupling strategy to obtain physically relevant stellar models. Casadio et al. [45] considered anisotropic compact model and isotropized it by varying the decoupling parameter involving in the MGD technique. Maurya et al. [46] adopted the no complexity constraint and checked the effect of the decoupling parameter on the developed embedding class-one model. Sharif and Majid [47] also formulated such models in Brans-Dicke theory and found them stable for certain parametric values.

In this article, we investigate how two different solutions representing compact models are affected by the charge as well as modified corrections of $f(\mathbb{R}, \mathbb{T})$ gravity. Following lines depict how this paper is organized. We introduce some basic foundations of the modified theory and formulate the corresponding field equations in the presence of charge as well as an extra matter source in section **2**. Section **3** separates these equations into two sets through the MGD scheme. Two different constraints depending on the matter sector are adopted in sections **4** and **5**, leading to the resulting solutions. Section **6** analyzes the corresponding matter determinants and other physical characteristics to check whether the modified models are physically relevant or not. Lastly, section **7** sums up our results.

2 $f(\mathbb{R}, \mathbb{T})$ Gravity

The presence of an additional source in the gravitational field modifies the Einstein-Hilbert action (with $\kappa = 8\pi$) in the following form [6]

$$S = \int \sqrt{-g} \left[\frac{f(\mathbb{R}, \mathbb{T})}{16\pi} + \mathbb{L}_m + \mathbb{L}_E + \gamma \mathbb{L}_c \right] d^4x, \quad (1)$$

where \mathbb{L}_c being the Lagrangian density of an extra source gravitationally coupled to the original field, \mathbb{L}_m and \mathbb{L}_E are that of the matter distribution

and an electromagnetic field, respectively. Also, the determinant of the metric tensor $g_{\beta\alpha}$ is symbolized by g . Taking the action (1) and applying the principle of least-action produces the field equations as

$$\mathbb{G}_{\beta\alpha} = 8\pi\mathbb{T}_{\beta\alpha}^{(\text{total})}, \quad (2)$$

where $\mathbb{G}_{\beta\alpha}$ being an Einstein tensor that describes the geometry of the space-time whereas the interior fluid distribution is characterized by the right hand side of the above equation. We further classify it for the current scenario as

$$\mathbb{T}_{\beta\alpha}^{(\text{total})} = \mathbb{T}_{\beta\alpha}^{(\text{ef})} + \gamma\mathfrak{C}_{\beta\alpha} = \frac{1}{f_{\mathbb{R}}}(\mathbb{T}_{\beta\alpha} + \mathbb{E}_{\beta\alpha}) + \mathbb{T}_{\beta\alpha}^{(\text{D})} + \gamma\mathfrak{C}_{\beta\alpha}, \quad (3)$$

where $f_{\mathbb{R}} = \frac{\partial f(\mathbb{R}, \mathbb{T})}{\partial \mathbb{R}}$. Moreover, γ controls the effect of an additional matter sector ($\mathfrak{C}_{\beta\alpha}$) on the seed interior configuration of celestial systems, and we call it the decoupling parameter. The modification in the Einstein-Hilbert action results in the effective EMT, denoted by $\mathbb{T}_{\beta\alpha}^{(\text{ef})}$ containing the usual matter part of $\mathbb{G}\mathbb{R}$ (in which $\mathbb{T}_{\beta\alpha}$ and $\mathbb{E}_{\beta\alpha}$ being the usual and electromagnetic EMTs, respectively) and correction terms $\mathbb{T}_{\beta\alpha}^{(\text{D})}$ of the extended theory. The later term has the form

$$\begin{aligned} \mathbb{T}_{\beta\alpha}^{(\text{D})} &= \frac{1}{8\pi f_{\mathbb{R}}} \left[\mathbb{T}_{\beta\alpha} f_{\mathbb{T}} + \left\{ \frac{1}{2}(f - \mathbb{R}f_{\mathbb{R}}) - \mathbb{L}_m f_{\mathbb{T}} \right\} g_{\beta\alpha} \right. \\ &\quad \left. - (g_{\beta\alpha} \square - \nabla_{\beta} \nabla_{\alpha}) f_{\mathbb{R}} + 2g^{\rho\zeta} f_{\mathbb{T}} \frac{\partial^2 \mathbb{L}_m}{\partial g^{\beta\alpha} \partial g^{\rho\zeta}} \right], \end{aligned} \quad (4)$$

where $f_{\mathbb{T}} = \frac{\partial f(\mathbb{R}, \mathbb{T})}{\partial \mathbb{T}}$. Also, the term ∇_{β} being the covariant derivative and $\square \equiv \frac{1}{\sqrt{-g}} \partial_{\beta} (\sqrt{-g} g^{\beta\alpha} \partial_{\alpha})$ is the D'Alembertian operator.

We shall discuss the complexity of a self-gravitating system, therefore, the nature of seed fluid distribution must be anisotropic. The following EMT represents such kind of fluids as

$$\mathbb{T}_{\beta\alpha} = \mu \mathcal{K}_{\beta} \mathcal{K}_{\alpha} + P_{\perp} (\mathcal{K}_{\beta} \mathcal{K}_{\alpha} + g_{\beta\alpha} - \mathcal{W}_{\beta} \mathcal{W}_{\alpha}) + P_r \mathcal{W}_{\beta} \mathcal{W}_{\alpha}, \quad (5)$$

where the triplet (P_r, P_{\perp}, μ) symbolizes the radial/tangential pressure and density, respectively. Further, \mathcal{K}_{β} being the four-velocity and \mathcal{W}_{β} is the four-vector satisfying the following relations

$$\mathcal{W}^{\beta} \mathcal{K}_{\beta} = 0, \quad \mathcal{W}^{\beta} \mathcal{W}_{\beta} = 1, \quad \mathcal{K}^{\beta} \mathcal{K}_{\beta} = -1.$$

Further, the expression for $\mathbb{E}_{\beta\alpha}$ is provided by

$$\mathbb{E}_{\beta\alpha} = -\frac{1}{4\pi} \left[\frac{1}{4} g_{\beta\alpha} \mathbb{F}^{\zeta\eta} \mathbb{F}_{\zeta\eta} - \mathbb{F}_{\beta}^{\zeta} \mathbb{F}_{\alpha\zeta} \right].$$

Here, the Maxwell field tensor is defined as $\mathbb{F}_{\zeta\eta} = \Phi_{\eta;\zeta} - \Phi_{\zeta;\eta}$ with $\Phi_{\zeta} = \Phi(r)\delta_{\zeta}^0$ being the four-potential. A concise form of the Maxwell equations is presented in the following

$$\mathbb{F}_{;\eta}^{\zeta\eta} = 4\pi j^{\zeta}, \quad \mathbb{F}_{[\zeta\eta;\alpha]} = 0, \quad (6)$$

where $j^{\zeta} = \Omega \mathcal{K}^{\zeta}$ and Ω being the current and charge densities, respectively.

The extended field equations (2) have the following trace given by

$$(\mathbb{R} + 3\nabla^{\beta}\nabla_{\beta})f_{\mathbb{R}} - \mathbb{T} + (\mathbb{T} + 4\mathbb{L}_m)f_{\mathbb{T}} - 2f - 2f_{\mathbb{T}}g^{\rho\zeta}g^{\beta\alpha}\frac{\partial^2\mathbb{L}_m}{\partial g^{\rho\zeta}\partial g^{\beta\alpha}} = 0.$$

By taking the vacuum case into account, we can retrieve the $f(\mathbb{R}, \mathbb{T})$ equations of motion and their solutions to $f(\mathbb{R})$ gravitational theory. The co-variant divergence of effective $\mathbb{E}\mathbb{M}\mathbb{T}$ is zero, however, that of usual matter distribution is non-null due to the inclusion of the curvature-matter coupling in the gravitational action. Consequently, an additional force comes into existence that can be seen from the following expression

$$\begin{aligned} \nabla^{\beta}\mathbb{T}_{\beta\alpha} = & \frac{f_{\mathbb{T}}}{8\pi - f_{\mathbb{T}}} \left[(\mathbb{T}_{\beta\alpha} + \Theta_{\beta\alpha})\nabla^{\beta}\ln f_{\mathbb{T}} + \nabla^{\beta}\Theta_{\beta\alpha} \right. \\ & \left. - \frac{8\pi\gamma}{f_{\mathbb{T}}}\nabla^{\beta}\mathbf{e}_{\beta\alpha} - \frac{1}{2}g_{\rho\zeta}\nabla_{\alpha}\mathbb{T}^{\rho\zeta} - \frac{8\pi}{f_{\mathbb{T}}}\nabla^{\beta}\mathbb{E}_{\beta\alpha} \right], \end{aligned} \quad (7)$$

where $\Theta_{\beta\alpha} = g_{\beta\alpha}\mathbb{L}_m - 2\mathbb{T}_{\beta\alpha} - 2g^{\rho\zeta}\frac{\partial^2\mathbb{L}_m}{\partial g^{\beta\alpha}\partial g^{\rho\zeta}}$. Several choices of the matter Lagrangian have been analyzed in the literature for isotropic/anisotropic fluids including the energy density, pressure, torsion, etc. Since we consider the anisotropic matter distribution, $\mathbb{L}_m = P = \frac{2P_{\perp} + P_r}{3}$ is the most suitable choice in this case [6].

A self-gravitating geometry can be distinguished into an interior and exterior regions by the hypersurface Σ . We define the interior region of a static spherical spacetime by the following line element as

$$ds^2 = -e^{x_1}dt^2 + e^{x_2}dr^2 + r^2d\vartheta^2 + r^2\sin^2\vartheta d\varphi^2, \quad (8)$$

where $\chi_1 = \chi_1(r)$ and $\chi_2 = \chi_2(r)$. The two quantities \mathcal{W}_β and \mathcal{K}_β in Eq.(5) become in terms of the above metric as

$$\mathcal{W}_\beta = (0, e^{\frac{\chi_2}{2}}, 0, 0), \quad \mathcal{K}_\beta = (-e^{\frac{\chi_1}{2}}, 0, 0, 0).$$

Further, Eq.(6) (left) now leads to the following differential equation

$$\Phi'' - \frac{1}{2r} \{r(\chi_1' + \chi_2') - 4\} \Phi' = 4\pi\Omega e^{\frac{\chi_1}{2} + \chi_2}, \quad (9)$$

whose integration yields

$$\Phi' = \frac{s(r)}{r^2} e^{\frac{\chi_1 + \chi_2}{2}}, \quad (10)$$

where $' = \frac{\partial}{\partial r}$ and $s(r) = \int_0^r \Omega e^{\frac{\chi_2}{2}} \hat{r}^2 d\hat{r}$ being the total interior charge.

We shall present a graphical analysis of the resulting solutions (will be developed in the later sections), thus it is necessary to adopt a specific model that can help us to express our results meaningfully. Several matter-geometry coupled $f(\mathbb{R}, \mathbb{T})$ models have been studied in the literature. Since we aim to find our solutions through the gravitational decoupling strategy, a very useful linear model in this regard is assumed in the following

$$f(\mathbb{R}, \mathbb{T}) = f_1(\mathbb{R}) + f_2(\mathbb{T}) = \mathbb{R} + 2\chi_3\mathbb{T}, \quad (11)$$

where $\mathbb{T} = P_r + 2P_\perp - \mu$ and χ_3 being a real-valued coupling constant. We have employed this model to construct two different anisotropic solutions and observed our results consistent with \mathbb{GR} [48].

The line element (8) and modified model (11) produce the non-zero components of the field equations (2) as

$$8\pi (\mu - \gamma \mathfrak{E}_0^0) + \frac{s^2}{r^4} = e^{-\chi_2} \left(\frac{\chi_2'}{r} - \frac{1}{r^2} \right) + \frac{1}{r^2} - \chi_3 \left(3\mu - \frac{P_r}{3} - \frac{2P_\perp}{3} \right), \quad (12)$$

$$8\pi (P_r + \gamma \mathfrak{E}_1^1) - \frac{s^2}{r^4} = e^{-\chi_2} \left(\frac{1}{r^2} + \frac{\chi_1'}{r} \right) - \frac{1}{r^2} + \chi_3 \left(\mu - \frac{7P_r}{3} - \frac{2P_\perp}{3} \right), \quad (13)$$

$$8\pi (P_\perp + \gamma \mathfrak{E}_2^2) + \frac{s^2}{r^4} = \frac{e^{-\chi_2}}{4} \left(\chi_1'^2 - \chi_2'\chi_1' + 2\chi_1'' - \frac{2\chi_2'}{r} + \frac{2\chi_1'}{r} \right) + \chi_3 \left(\mu - \frac{P_r}{3} - \frac{8P_\perp}{3} \right), \quad (14)$$

where the entities along by χ_3 on the right side of above equations appear due to $f(\mathbb{R}, \mathbb{T})$ corrections. Moreover, Eq.(7) together with (11) takes the form

$$\begin{aligned} \frac{dP_r}{dr} + \frac{\chi'_1}{2}(\mu + P_r) + \frac{\gamma\chi'_1}{2}(\mathfrak{e}_1^1 - \mathfrak{e}_0^0) + \frac{2}{r}(P_r - P_\perp) \\ + \gamma\frac{d\mathfrak{e}_1^1}{dr} + \frac{2\gamma}{r}(\mathfrak{e}_1^1 - \mathfrak{e}_2^2) = \frac{1}{\chi_3 - 4\pi} \left\{ \chi_3(\mu' - P') - \frac{ss'}{4\pi r^4} \right\}. \end{aligned} \quad (15)$$

We can call Eq.(15) as the generalized Tolman-Oppenheimer-Volkoff equation that contains different forces such as Newtonian, hydrodynamical, the gravitational and extra force due to modified gravity. This equation further helps to study fluctuations in a self-gravitating structure due to different factors.

3 Gravitational Decoupling

Since the inclusion of a new gravitational source increases unknowns in the field equations, i.e., $(\chi_1, \chi_2, s, \mu, P_\perp, P_r, \mathfrak{e}_0^0, \mathfrak{e}_1^1, \mathfrak{e}_2^2)$, an analytical solution to this highly non-linear set of equations is not possible unless we employ different constraints. On that note, a systematic scheme (termed as the gravitational decoupling [27]) is employed so that the modified field equations can be made solvable. An interesting point is that this strategy transforms the metric components and leads the field equations to a new framework where they can easily be solved. The following solution to Eqs.(12)-(14) is now considered to execute this technique given by

$$ds^2 = -e^{\chi_4(r)} dt^2 + \frac{1}{\chi_5(r)} dr^2 + r^2 d\vartheta^2 + r^2 \sin^2 \vartheta d\varphi^2. \quad (16)$$

The linear transformations of the metric components are presented by

$$\chi_4 \rightarrow \chi_1 = \chi_4 + \gamma t, \quad \chi_5 \rightarrow e^{-\chi_2} = \chi_5 + \gamma f, \quad (17)$$

where t being the temporal and f is the radial deformation function. We strive to deform only the g_{rr} component, thus MGD scheme is chosen to be applied that preserves the temporal metric function, i.e., $f \rightarrow \bar{\mathcal{F}}$, $t \rightarrow 0$. Eq.(17) then switches into

$$\chi_4 \rightarrow \chi_1 = \chi_4, \quad \chi_5 \rightarrow e^{-\chi_2} = \chi_5 + \gamma \bar{\mathcal{F}}, \quad (18)$$

where $\bar{\mathcal{F}} = \bar{\mathcal{F}}(r)$. It must be noted that such kind of linear mappings does not disturb the symmetry of a sphere. The implementation of the transformation (18) on the system (12)-(14) leads to two distinct sets. The first of them (corresponding to $\gamma = 0$) represents the original (charged anisotropic) matter source given by

$$8\pi\mu + \chi_3 \left(3\mu - \frac{P_r}{3} - \frac{2P_\perp}{3} \right) + \frac{s^2}{r^4} = e^{-\chi_2} \left(\frac{\chi'_2}{r} - \frac{1}{r^2} \right) + \frac{1}{r^2}, \quad (19)$$

$$8\pi P_r - \chi_3 \left(\mu - \frac{7P_r}{3} - \frac{2P_\perp}{3} \right) - \frac{s^2}{r^4} = e^{-\chi_2} \left(\frac{1}{r^2} + \frac{\chi'_1}{r} \right) - \frac{1}{r^2}, \quad (20)$$

$$8\pi P_\perp - \chi_3 \left(\mu - \frac{P_r}{3} - \frac{8P_\perp}{3} \right) + \frac{s^2}{r^4} = \frac{e^{-\chi_2}}{4} \left(\chi_1'^2 - \chi_2' \chi_1' + 2\chi_1'' - \frac{2\chi_2'}{r} + \frac{2\chi_1'}{r} \right). \quad (21)$$

The explicit expressions for the triplet (μ, P_r, P_\perp) can be obtained by solving Eqs.(19)-(21) simultaneously as

$$\begin{aligned} \mu = & \frac{e^{-\chi_2}}{48r^4(\chi_3 + 2\pi)(\chi_3 + 4\pi)} \left[r^4 \chi_3 \chi_1'^2 + r^3 \chi_3 \chi_1' (4 - r\chi_2') + 2\{r^4 \chi_3 \chi_1'' \right. \\ & + 8r^3(\chi_3 + 3\pi)\chi_2' + 24\pi r^2 e^{\chi_2} + 8r^2 \chi_3 e^{\chi_2} - 8r^2 \chi_3 - 10s^2 \chi_3 e^{\chi_2} \\ & \left. - 24\pi r^2 - 24\pi s^2 e^{\chi_2} \right], \end{aligned} \quad (22)$$

$$\begin{aligned} P_r = & \frac{e^{-\chi_2}}{48r^4(\chi_3 + 2\pi)(\chi_3 + 4\pi)} \left[r^3 \chi_1' (r\chi_3 \chi_2' + 20\chi_3 + 48\pi) - 2r^4 \chi_3 \chi_1'' \right. \\ & - r^4 \chi_3 \chi_1'^2 + 8r^3 \chi_3 \chi_2' - 48\pi r^2 e^{\chi_2} - 16r^2 \chi_3 e^{\chi_2} + 16r^2 \chi_3 + 20s^2 \chi_3 e^{\chi_2} \\ & \left. + 48\pi r^2 + 48\pi s^2 e^{\chi_2} \right], \end{aligned} \quad (23)$$

$$\begin{aligned} P_\perp = & \frac{e^{-\chi_2}}{48r^4(\chi_3 + 2\pi)(\chi_3 + 4\pi)} \left[r^4 (5\chi_3 + 12\pi) \chi_1'^2 + r^3 \chi_1' (8(\chi_3 + 3\pi) \right. \\ & - r(5\chi_3 + 12\pi)\chi_2') - 2\{2r^3(\chi_3 + 6\pi)\chi_2' - r^4(5\chi_3 + 12\pi)\chi_1'' + 4r^2 \chi_3 \\ & \left. - 4r^2 \chi_3 e^{\chi_2} + 24\pi s^2 e^{\chi_2} + 14s^2 \chi_3 e^{\chi_2} \right]. \end{aligned} \quad (24)$$

Furthermore, the second set (for $\gamma = 1$) encodes the effect of an additional source ($\mathfrak{E}_\alpha^\beta$) given by

$$8\pi \mathfrak{E}_0^0 = \frac{1}{r} \left(\bar{\mathcal{F}}' + \frac{\bar{\mathcal{F}}}{r} \right), \quad (25)$$

$$8\pi \mathfrak{E}_1^1 = \frac{\bar{\mathcal{F}}}{r} \left(\chi_1' + \frac{1}{r} \right), \quad (26)$$

$$8\pi\mathfrak{E}_2^2 = \frac{\bar{\mathcal{F}}}{4} \left(2\chi_1'' + \chi_1'^2 + \frac{2\chi_1'}{r} \right) + \frac{\bar{\mathcal{F}}'}{2} \left(\frac{\chi_1'}{2} + \frac{1}{r} \right). \quad (27)$$

Since we follow the MGD scheme, the energy exchange between both (seed and additional) matter distributions is not allowed and hence, they conserve individually. The decoupling of the system (12)-(14) into two sectors has successfully been done. It is observed that there are six unknowns $(\mu, P_r, P_\perp, s, \chi_1, \chi_2)$ in the first set of equations (22)-(24), therefore, we need a well-behaved solution and a known form of the electric charge to continue our analysis. On the other hand, the second sector (25)-(27) contains four unknowns $(\bar{\mathcal{F}}, \mathfrak{E}_0^0, \mathfrak{E}_1^1, \mathfrak{E}_2^2)$ and remains the same as that of an uncharged scenario. In this regard, the only constraint will be needed on \mathfrak{E} -sector to close the system. Following equations help to detect the effective matter determinants as

$$\bar{\mu} = \mu - \gamma\mathfrak{E}_0^0, \quad \bar{P}_r = P_r + \gamma\mathfrak{E}_1^1, \quad \bar{P}_\perp = P_\perp + \gamma\mathfrak{E}_2^2, \quad (28)$$

and the total anisotropy produced in the system becomes

$$\bar{\Pi} = \bar{P}_\perp - \bar{P}_r = (P_\perp - P_r) + \gamma(\mathfrak{E}_2^2 - \mathfrak{E}_1^1) = \Pi + \Pi_{\mathfrak{E}}, \quad (29)$$

where Π and $\Pi_{\mathfrak{E}}$ being the anisotropy of the seed and additional sources, respectively.

4 Isotropization of Compact Sources

Since $\bar{\Pi}$ shows the total anisotropy of the spherical geometry triggered by both seed and extra matter sources which may be different from that of caused only by the initial source $\mathbb{T}_{\beta\alpha}$, i.e., Π . This section discusses the conversion of the anisotropic system into an isotropic geometry when a new matter source is included. This can mathematically be justified by $\bar{\Pi} = 0$. We shall show in the following lines that how the variation in the decoupling parameter affects (or controls) such evolutionary change. It is observed that the system is anisotropic for $\gamma = 0$ and isotropic when $\gamma = 1$. Since we discuss the later case that yields from Eq.(29) as

$$\Pi_{\mathfrak{E}} = -\Pi \quad \Rightarrow \quad \mathfrak{E}_2^2 - \mathfrak{E}_1^1 = P_r - P_\perp. \quad (30)$$

This condition has been widely used to make the system isotropic from being anisotropic through minimal/extended decoupling schemes [45, 48]. A

particular acceptable ansatz is now considered in the following so that the number of unknowns can be decreased. This is given by

$$\chi_1(r) = \ln \left\{ \mathcal{C}_2^2 \left(1 + \frac{r^2}{\mathcal{C}_1^2} \right) \right\}, \quad (31)$$

$$\chi_5(r) = e^{-\chi_2} = \frac{\mathcal{C}_1^2 + r^2}{\mathcal{C}_1^2 + 3r^2}, \quad (32)$$

leading the matter variables to

$$\begin{aligned} \mu = & \frac{1}{12r^4(\chi_3 + 2\pi)(\chi_3 + 4\pi)(\mathcal{C}_1^2 + 3r^2)^2} [3\mathcal{C}_1^2 r^2(\chi_3(9r^2 - 10s^2) \\ & + 24\pi(r^2 - s^2)) - \mathcal{C}_1^4 s^2(5\chi_3 + 12\pi) + 3r^4(5\chi_3 + 12\pi)(2r^2 - 3s^2)], \end{aligned} \quad (33)$$

$$\begin{aligned} P_r = & \frac{1}{12r^4(\chi_3 + 2\pi)(\chi_3 + 4\pi)(\mathcal{C}_1^2 + 3r^2)^2} [3\mathcal{C}_1^2 r^2(3r^2\chi_3 + 10s^2\chi_3 \\ & + 24\pi s^2) + \mathcal{C}_1^4 s^2(5\chi_3 + 12\pi) + 3r^4(2r^2\chi_3 + 15s^2\chi_3 + 36\pi s^2)], \end{aligned} \quad (34)$$

$$\begin{aligned} P_\perp = & \frac{1}{12r^4(\chi_3 + 2\pi)(\chi_3 + 4\pi)(\mathcal{C}_1^2 + 3r^2)^2} [3\mathcal{C}_1^2 r^2(3r^2\chi_3 - 14s^2\chi_3 \\ & - 24\pi s^2) - \mathcal{C}_1^4 s^2(7\chi_3 + 12\pi) + 3r^4(\chi_3(8r^2 - 21s^2) + 12\pi(r^2 - 3s^2))], \end{aligned} \quad (35)$$

where \mathcal{C}_1^2 and \mathcal{C}_2^2 are unknowns that shall later be determined through continuity of the metric functions. Some clusters of different particles move in randomly oriented (circular-like) orbits in their gravitational field. The above considered solution (31) and (32) helps to determine such fields [49]. Casadio et al. [45] also used them to formulate the decoupled anisotropic solution in \mathbb{GR} .

An important topic of all time for researchers is the junction conditions which help them to analyze several significant characteristics of celestial structures at the surface of a sphere, i.e., $\Sigma : r = \mathcal{R}$. We need to consider an exterior metric representing vacuum spacetime so that the smooth matching can be done. Since our considered model (11) is equivalent to \mathbb{GR} in a vacuum, we take the exterior solution provided by the Reissner-Nordström line element given by

$$ds^2 = - \left(1 - \frac{2\bar{\mathcal{M}}}{r} + \frac{\bar{\mathcal{S}}^2}{r^2} \right) dt^2 + \frac{1}{\left(1 - \frac{2\bar{\mathcal{M}}}{r} + \frac{\bar{\mathcal{S}}^2}{r^2} \right)} dr^2 + r^2 d\vartheta^2 + r^2 \sin^2 \vartheta d\varphi^2, \quad (36)$$

where $\bar{\mathcal{S}}$ and $\bar{\mathcal{M}}$ being the total charge and mass, respectively. The constants \mathcal{C}_1^2 and \mathcal{C}_2^2 are obtained as

$$\mathcal{C}_1^2 = \frac{\mathcal{R}^2(2\mathcal{R}^2 - 6\bar{\mathcal{M}}\mathcal{R} + 3\bar{\mathcal{S}}^2)}{2\bar{\mathcal{M}}\mathcal{R} - \bar{\mathcal{S}}^2}, \quad (37)$$

$$\mathcal{C}_2^2 = \frac{2\mathcal{R}^2 - 6\bar{\mathcal{M}}\mathcal{R} + 3\bar{\mathcal{S}}^2}{2\mathcal{R}^2}. \quad (38)$$

We consider a particular compact star $4U\ 1820 - 30$ with a radius $\mathcal{R} = 9.1 \pm 0.4 km$ and mass $\bar{\mathcal{M}} = 1.58 \pm 0.06 M_\odot$ (M_\odot being mass of the sun) to graphically analyze the physical characteristics of the anisotropic models [50]. This is a unique compact X-ray binary in the globular cluster NGC 6624 that exhibits significant luminosity variability and an extremely short orbital period of 685s. Joining together the constraint (30), a known form of the charge (involving a constant χ_6 [36]), the modified field equations and the considered metric potentials (31)-(32) result in a first-order differential equation as

$$\begin{aligned} & r(\mathcal{C}_1^2 + r^2) \{ 8\pi r^3 (\mathcal{C}_1^2 + r^2) (2\chi_6 \mathcal{C}_1^4 + 12\chi_6 \mathcal{C}_1^2 r^2 + 18\chi_6 r^4 - 3) \\ & - (\chi_3 + 4\pi) (\mathcal{C}_1^2 + 2r^2) (\mathcal{C}_1^2 + 3r^2)^2 \mathcal{F}'(r) \} + 2(\chi_3 + 4\pi) \\ & \times (\mathcal{C}_1^4 + 2\mathcal{C}_1^2 r^2 + 2r^4) (\mathcal{C}_1^2 + 3r^2)^2 \mathcal{F}(r) = 0. \end{aligned} \quad (39)$$

Integrating the above equation for the deformation function $\mathcal{F}(r)$, we get

$$\mathcal{F}(r) = \frac{r^2(\mathcal{C}_1^2 + r^2)}{\mathcal{C}_1^2 + 2r^2} \left[\mathbb{C}_1 + \frac{8\pi}{(\chi_3 + 4\pi)} \left\{ \frac{\chi_6 \mathcal{C}_1^2}{3} + \frac{1}{2\mathcal{C}_1^2 + 6r^2} + \chi_6 r^2 \right\} \right], \quad (40)$$

with \mathbb{C}_1 being a real-valued constant. Equation (40) produces the deformed g_{rr} component as

$$\begin{aligned} e^{\chi_2} = \chi_5^{-1} = & [(\mathcal{C}_1^2 + r^2) \{ 3\mathcal{C}_1^2 (\chi_3 + 4\pi) (\gamma \mathbb{C}_1 r^2 + 1) + 3r^2 (\chi_3 (3\gamma \mathbb{C}_1 r^2 + 2) \\ & + 4\pi (3\gamma \mathbb{C}_1 r^2 + \gamma + 2)) + 8\pi \gamma r^2 \chi_6 (\mathcal{C}_1^2 + 3r^2)^2 \}]^{-1} [3(\chi_3 + 4\pi) \\ & \times (5\mathcal{C}_1^2 r^2 + \mathcal{C}_1^4 + 6r^4)]. \end{aligned} \quad (41)$$

Hence, the following line element represents minimally deformed anisotropic solution to the Eqs.(12)-(14) given by

$$ds^2 = -\mathcal{C}_2^2 \left(1 + \frac{r^2}{\mathcal{C}_1^2} \right) dt^2 + \frac{\mathcal{C}_1^2 + 3r^2}{\mathcal{C}_1^2 + r^2 + \alpha \mathcal{F}(\mathcal{C}_1^2 + 3r^2)} dr^2 + r^2 d\vartheta^2 + r^2 \sin^2 \vartheta d\varphi^2, \quad (42)$$

and the respective state determinants are presented as

$$\begin{aligned}
\bar{\mu} &= \frac{-1}{24\pi(\chi_3 + 2\pi)(\chi_3 + 4\pi)(\mathcal{C}_1^2 + 2r^2)^2(\mathcal{C}_1^2 + 3r^2)^2} \\
&\times [\mathcal{C}_1^8\{9\gamma\mathbb{C}_1\chi_3^2 + 2\pi\chi_3(27\gamma\mathbb{C}_1 + 5(32\gamma + 1)r^2\chi_6) + 8\pi^2((80\gamma + 3)r^2\chi_6 \\
&+ 9\gamma\mathbb{C}_1)\} + \mathcal{C}_1^6\{75\gamma\mathbb{C}_1r^2\chi_3^2 + 2\pi\chi_3(9(25\gamma\mathbb{C}_1r^2 + 2\gamma - 3) + 2(408\gamma + 25) \\
&\times r^4\chi_6) + 24\pi^2(25\gamma\mathbb{C}_1r^2 + 3\gamma + 2(68\gamma + 5)r^4\chi_6 - 6)\} + \mathcal{C}_1^4r^2\{2\pi\chi_3 \\
&\times (675\gamma\mathbb{C}_1r^2 + 60\gamma + (1992\gamma + 185)r^4\chi_6 - 138) + 225\gamma\mathbb{C}_1r^2\chi_3^2 + 24\pi^2 \\
&\times (5(15\gamma\mathbb{C}_1r^2 + 2\gamma - 6) + (332\gamma + 37)r^4\chi_6)\} + 3\mathcal{C}_1^2r^4\{99\gamma\mathbb{C}_1r^2\chi_3^2 + 2\pi\chi_3 \\
&\times (9\gamma(33\mathbb{C}_1r^2 + 2) + 20(39\gamma + 5)r^4\chi_6 - 76) + 24\pi^2(\gamma(33\mathbb{C}_1r^2 + 3) + 10 \\
&\times (13\gamma + 2)r^4\chi_6 - 16)\} + 6r^6\{27\gamma\mathbb{C}_1r^2\chi_3^2 + 2\pi\chi_3(81\gamma\mathbb{C}_1r^2 + 6\gamma + 30r^4\chi_6 \\
&\times (6\gamma + 1) - 20) + 24\pi^2(9\gamma\mathbb{C}_1r^2 + \gamma + 6(5\gamma + 1)r^4\chi_6 - 4)\} + 24\pi\gamma\mathcal{C}_1^{10} \\
&\times (\chi_3 + 2\pi)\chi_6], \tag{43}
\end{aligned}$$

$$\begin{aligned}
\bar{P}_r &= \frac{1}{24\pi(\chi_3 + 2\pi)(\chi_3 + 4\pi)(\mathcal{C}_1^2 + 2r^2)(\mathcal{C}_1^2 + 3r^2)^2} \\
&\times [(\chi_3 + 2\pi)(\mathcal{C}_1^2 + 3r^2)^2\{3\gamma(\mathbb{C}_1\mathcal{C}_1^2(\chi_3 + 4\pi) + 3\mathbb{C}_1r^2\chi_3 + 4(3\pi\mathbb{C}_1r^2 + \pi)) \\
&+ 8\pi\gamma\chi_6(\mathcal{C}_1^2 + 3r^2)^2\} + 2\pi(\mathcal{C}_1^2 + 2r^2)\{r^2(5\chi_3 + 12\pi)\chi_6(\mathcal{C}_1^2 + 3r^2)^2 \\
&+ 3\chi_3(3\mathcal{C}_1^2 + 2r^2)\}], \tag{44}
\end{aligned}$$

$$\begin{aligned}
\bar{P}_\perp &= \frac{1}{24\pi(\chi_3 + 2\pi)(\chi_3 + 4\pi)(\mathcal{C}_1^2 + 2r^2)(\mathcal{C}_1^2 + 3r^2)^2} \\
&\times [\mathcal{C}_1^6\{3\gamma\mathbb{C}_1(\chi_3 + 2\pi)(\chi_3 + 4\pi) + 2\pi r^2\chi_6((60\gamma - 7)\chi_3 + 12\pi(10\gamma - 1))\} \\
&+ \mathcal{C}_1^4\{27\gamma\mathbb{C}_1r^2\chi_3^2 + 2\pi\chi_3(81\gamma\mathbb{C}_1r^2 + 6\gamma + 8(39\gamma - 7)r^4\chi_6 + 9) + 24\pi^2 \\
&\times (9\gamma\mathbb{C}_1r^2 + \gamma + 4(13\gamma - 2)r^4\chi_6)\} + 3\mathcal{C}_1^2r^2\{27\gamma\mathbb{C}_1r^2\chi_3^2 + 2\pi\chi_3(81\gamma\mathbb{C}_1r^2 \\
&+ 6\gamma + (228\gamma - 49)r^4\chi_6 + 14) + 24\pi^2(9\gamma\mathbb{C}_1r^2 + \gamma + (38\gamma - 7)r^4\chi_6 + 1)\} \\
&+ 3r^4\{27\gamma\mathbb{C}_1r^2\chi_3^2 + 2\pi\chi_3(81\gamma\mathbb{C}_1r^2 + 6\gamma + 6(30\gamma - 7)r^4\chi_6 + 16) + 24\pi^2 \\
&\times (9\gamma\mathbb{C}_1r^2 + \gamma + 6(5\gamma - 1)r^4\chi_6 + 2)\} + 8\pi\gamma\mathcal{C}_1^8(\chi_3 + 2\pi)\chi_6]. \tag{45}
\end{aligned}$$

Moreover, the pressure anisotropy corresponding to metric (42) is

$$\bar{\Pi} = \frac{r^2\{3 - 2\chi_6(\mathcal{C}_1^2 + 3r^2)^2\}(1 - \gamma)}{2(\chi_3 + 4\pi)(\mathcal{C}_1^2 + 3r^2)^2}, \tag{46}$$

from which we clearly observe that this factor disappears when $\gamma = 1$, hence, the considered matter source becomes isotropic for this parametric value.

Equations (43)-(46) provide the exact solution of $f(\mathbb{R}, \mathbb{T})$ field equations where γ belongs to $[0, 1]$. In this way, we can thoroughly follow the process of isotropizing the anisotropic fluid by taking variation in the decoupling parameter.

5 Complexity of Compact Sources

The notion of complexity was initially formulated for a static sphere [40] and then extended to the framework of dissipative dynamical matter configuration [41]. The basic idea to establish its definition is that there does not exist any factor that produces complexity in uniform/isotropic distribution. A specific factor that measures the complexity of a spacetime structure (i.e., \mathbb{Y}_{TF}) is one of the four different scalars resulting from the orthogonal decomposition of the curvature tensor. By following Herrera's technique, we obtain this scalar factor possessing $f(\mathbb{R}, \mathbb{T})$ corrections in the following form

$$\mathbb{Y}_{TF}(r) = (1 + \chi_3) \left(8\pi\Pi + \frac{2s^2}{r^4} \right) - \frac{4\pi}{r^3} \int_0^r \hat{r}^3 \mu'(\hat{r}) d\hat{r}. \quad (47)$$

The presence of an additional source in the current setup (12)-(14) makes the above complexity factor as

$$\begin{aligned} \bar{\mathbb{Y}}_{TF}(r) &= (1 + \chi_3) \left(8\pi\bar{\Pi} + \frac{2s^2}{r^4} \right) - \frac{4\pi}{r^3} \int_0^r \hat{r}^3 \bar{\mu}'(\hat{r}) d\hat{r} \\ &= (1 + \chi_3) \left(8\pi\Pi + \frac{2s^2}{r^4} \right) - \frac{4\pi}{r^3} \int_0^r \hat{r}^3 \mu'(\hat{r}) d\hat{r} \\ &+ 8\pi\Pi_{\mathfrak{C}}(1 + \chi_3) + \frac{4\pi}{r^3} \int_0^r \hat{r}^3 \mathfrak{C}_0'(\hat{r}) d\hat{r}. \end{aligned} \quad (48)$$

We can analogously write the above equation as

$$\bar{\mathbb{Y}}_{TF} = \mathbb{Y}_{TF} + \mathbb{Y}_{TF}^{\mathfrak{C}}, \quad (49)$$

where the sets (22)-(24) and (25)-(27) being represented by \mathbb{Y}_{TF} and $\mathbb{Y}_{TF}^{\mathfrak{C}}$, respectively. Since the model (43)-(46) is established for the constraint $\bar{\Pi} = 0$, Eq.(48) thus yields

$$\bar{\mathbb{Y}}_{TF} = \frac{2s^2}{r^4} (1 + \chi_3) - \frac{4\pi}{r^3} \int_0^r \hat{r}^3 \bar{\mu}'(\hat{r}) d\hat{r}. \quad (50)$$

Eq.(50) produces the following complexity factor after combining with the metric (42) and the modified field equations as

$$\begin{aligned}
\bar{\mathbb{Y}}_{TF} = & 2\chi_6 r^2(1 + \chi_3) + \frac{1}{30r^3(\chi_3 + 2\pi)(\chi_3 + 4\pi)(\mathcal{C}_1^2 + 2r^2)^2(\mathcal{C}_1^2 + 3r^2)^2} \\
& \times \left[\pi\mathcal{C}_1^8 r \{5\chi_3(4r^4(8\chi_6\gamma + \chi_6) + 3) + 16\pi\chi_6(20\gamma + 3)r^4\} + 5\mathcal{C}_1^6 \{48\pi^2 \right. \\
& \times (2r^7(6\chi_6\gamma + \chi_6) - \gamma\mathcal{C}_1 r^5) - 6\gamma\mathcal{C}_1 r^5 \chi_3^2 + \pi r^3 \chi_3(27 - 36\gamma\mathcal{C}_1 r^2 + 8\chi_6 \\
& \times (36\gamma + 5)r^4)\} + 4\mathcal{C}_1^4 r^5 \{-45\gamma\mathcal{C}_1 r^2 \chi_3^2 + 5\pi\chi_3(24(2 - \gamma) - 54\gamma\mathcal{C}_1 r^2 \\
& + \chi_6(240\gamma + 37)r^4) + 12\pi^2(30 - 20\gamma - 30\gamma\mathcal{C}_1 r^2 + \chi_6(200\gamma + 37)r^4)\} \\
& - 5\sqrt{3}\pi\sqrt{\mathcal{C}_1^2}\chi_3(\mathcal{C}_1^4 + 5\mathcal{C}_1^2 r^2 + 6r^4)^2 \tan^{-1}\left(\frac{\sqrt{3}r}{\sqrt{\mathcal{C}_1^2}}\right) + 30\mathcal{C}_1^2 r^7 \{2\pi\chi_3 \\
& \times (45 - 24\gamma - 27\gamma\mathcal{C}_1 r^2 + 20r^4(6\chi_6\gamma + \chi_6)) - 9\gamma\mathcal{C}_1 r^2 \chi_3^2 + 24\pi^2(8 - 4\gamma \\
& - 3\gamma\mathcal{C}_1 r^2 + 4r^4(5\chi_6\gamma + \chi_6))\} + 48\pi r^9 \{5\chi_3(10 - 3\gamma + 3r^4(6\chi_6\gamma + \chi_6)) \\
& \left. + 6\pi(6r^4(5\chi_6\gamma + \chi_6) - 5(\gamma - 4))\} \right]. \tag{51}
\end{aligned}$$

5.1 Two Systems with the Same Complexity Factor

In this subsection, we consider that the scalar factor \mathbb{Y}_{TF} representing the complexity of an initial matter source does not possess any change when a new gravitational source $\mathfrak{C}_{\beta\alpha}$ is added, i.e., $\mathbb{Y}_{TF}^{\mathfrak{C}} = 0$. This constraint results in $\bar{\mathbb{Y}}_{TF} = \mathbb{Y}_{TF}$ or

$$8\pi\Pi_{\mathfrak{C}}(1 + \chi_3) = -\frac{4\pi}{r^3} \int_0^r \hat{r}^3 \mathfrak{C}_0^{0'}(\hat{r}) d\hat{r}. \tag{52}$$

We use Eq.(25) to manipulate the right side of (52) as

$$-\frac{4\pi}{r^3} \int_0^r \hat{r}^3 \mathfrak{C}_0^{0'}(\hat{r}) d\hat{r} = -\frac{1}{2r} \left(\mathcal{F}' - \frac{2\mathcal{F}}{r} \right), \tag{53}$$

yielding the condition (52) as the following first-order differential equation given by

$$(\chi_3 + 1) \left\{ \mathcal{F}'(r) \left(\frac{\chi_1'}{4} + \frac{1}{2r} \right) + \mathcal{F}(r) \left(\frac{\chi_1''}{2} - \frac{1}{r^2} + \frac{\chi_1'^2}{4} - \frac{\chi_1'}{2r} \right) \right\}$$

$$+\frac{1}{2r}\left(\mathcal{F}' - \frac{2\mathcal{F}}{r}\right) = 0. \quad (54)$$

This equation possesses the temporal metric function describing the original anisotropic matter field, hence increases the unknowns. The Tolman IV ansatz is used in this regard to make the system solvable as

$$\chi_1(r) = \ln \left\{ \mathcal{C}_2^2 \left(1 + \frac{r^2}{\mathcal{C}_1^2} \right) \right\}, \quad (55)$$

$$\chi_5(r) = e^{-\chi_2} = \frac{(\mathcal{C}_1^2 + r^2)(\mathcal{C}_3^2 - r^2)}{\mathcal{C}_3^2(\mathcal{C}_1^2 + 2r^2)}, \quad (56)$$

triggered by the density and pressure isotropy as

$$\begin{aligned} \mu = & \frac{1}{12\mathcal{C}_3^2(\chi_3 + 2\pi)(\chi_3 + 4\pi)(\mathcal{C}_1^2 + 2r^2)^2} \\ & \times [\mathcal{C}_1^4\{12(\chi_3 + 3\pi) - \chi_6\mathcal{C}_3^2r^2(5\chi_3 + 12\pi)\} + \mathcal{C}_1^2\{12r^2(2\chi_3 + 7\pi) - \mathcal{C}_3^2 \\ & \times (5\chi_3 + 12\pi)(4\chi_6r^4 - 3)\} + 2r^2\{9r^2(\chi_3 + 4\pi) - 2\mathcal{C}_3^2(5\chi_6r^4\chi_3 - 3\chi_3 \\ & + 12\pi\chi_6r^4 - 6\pi)\}], \end{aligned} \quad (57)$$

$$\begin{aligned} P = & \frac{1}{12\mathcal{C}_3^2(\chi_3 + 2\pi)(\chi_3 + 4\pi)(\mathcal{C}_1^2 + 2r^2)^2} \\ & \times [\mathcal{C}_1^4\{\chi_6\mathcal{C}_3^2r^2(5\chi_3 + 12\pi) - 12\pi\} + \mathcal{C}_1^2\{\mathcal{C}_3^2(20\chi_6r^4\chi_3 + 48\pi\chi_6r^4 + 12\pi \\ & + 9\chi_3) - 12r^2(\chi_3 + 5\pi)\} + 2r^2\{2\mathcal{C}_3^2\{5\chi_6r^4\chi_3 + 12\pi\chi_6r^4 + 3\chi_3 + 6\pi\} \\ & - 9r^2(\chi_3 + 4\pi)\}]. \end{aligned} \quad (58)$$

Equations (37) and (38) supply the unknowns \mathcal{C}_1^2 and \mathcal{C}_2^2 , whereas \mathcal{C}_3^2 has the following form

$$\mathcal{C}_3^2 = \frac{2\mathcal{R}^3(\bar{\mathcal{S}}^2 - 2\bar{\mathcal{M}}\mathcal{R} + \mathcal{R}^2)}{2\bar{\mathcal{M}}\bar{\mathcal{S}} - 4\bar{\mathcal{M}}^2\mathcal{R} + \bar{\mathcal{S}}\mathcal{R} + 2\bar{\mathcal{M}}\mathcal{R}^2}. \quad (59)$$

Insertion of g_{tt} metric component (55) in Eq.(54) gives

$$\mathcal{F}(r) = \frac{\mathbb{C}_2r^2(\mathcal{C}_1^2 + r^2)}{\mathcal{C}_1^2(2 + \chi_3) + r^2(2\chi_3 + 3)}, \quad (60)$$

involving \mathbb{C}_2 as a constant of integration. Consequently, the deformed expression of g_{rr} component becomes

$$e^{\chi_2} = \chi_5^{-1} = \frac{\mathcal{C}_3^2(\mathcal{C}_1^2 + 2r^2)}{(\mathcal{C}_1^2 + r^2)} \left\{ \mathcal{C}_3^2 + r^2 \left(\frac{\gamma\mathbb{C}_2\mathcal{C}_3^2(\mathcal{C}_1^2 + 2r^2)}{\mathcal{C}_1^2(2 + \chi_3) + r^2(2\chi_3 + 3)} - 1 \right) \right\}^{-1}, \quad (61)$$

and the total complexity factor $\bar{\mathbb{Y}}_{TF}$ defined in Eq.(48) leads to

$$\begin{aligned} \bar{\mathbb{Y}}_{TF} = \mathbb{Y}_{TF} = & \frac{1}{16r^3\mathcal{C}_3^2(\chi_3 + 2\pi)(\chi_3 + 4\pi)(\mathcal{C}_1^2 + 2r^2)^2} \left[2r \{ 45\pi\mathcal{C}_1^6\chi_3 \right. \\ & + 2\mathcal{C}_1^4(120\chi_6r^4\mathcal{C}_3^2\chi_3^2(\chi_3 + 1) + 96\pi^2\chi_6r^4\mathcal{C}_3^2 + 5\pi\chi_3(8(6\chi_3 + 7) \\ & \times \chi_6r^4\mathcal{C}_3^2 + 15r^2 + 9\mathcal{C}_3^2)) + 4\mathcal{C}_1^2(240\chi_6r^6\mathcal{C}_3^2\chi_3^2(\chi_3 + 1) + 5\pi r^2\chi_3 \\ & \times (16\chi_6r^4\mathcal{C}_3^2(6\chi_3 + 7) + 24r^2 + 15\mathcal{C}_3^2) + 48\pi^2r^4(4\chi_6r^2\mathcal{C}_3^2 + 5)) \\ & + 64r^4\mathcal{C}_3^2(15\chi_6r^4\chi_3^2(\chi_3 + 1) + 5\pi\chi_3(\chi_6r^4(6\chi_3 + 7) + 3) + 6\pi^2 \\ & \left. \times (2\chi_6r^4 + 5)) \} - 45\sqrt{2}\pi\sqrt{\mathcal{C}_1^2\chi_3}(\mathcal{C}_1^2 + 2r^2)^2(\mathcal{C}_1^2 + 2\mathcal{C}_3^2) \tan^{-1} \left(\frac{\sqrt{2}r}{\sqrt{\mathcal{C}_1^2}} \right) \right]. \end{aligned} \quad (62)$$

5.2 Constructing Solutions with Null Complexity

This subsection establishes a solution to the $f(\mathbb{R}, \mathbb{T})$ field equations for a particular constraint depending on the complexity factor. It is considered that the original anisotropic source does possess the complexity such that $\mathbb{Y}_{TF} \neq 0$, however, the system becomes free from complexity once a new gravitational source is added. This can mathematically be expressed by $\bar{\mathbb{Y}}_{TF} = 0$, that leads Eq.(49) in terms of ansatz (55) and (56) to

$$\begin{aligned} & \frac{120r(\chi_6 + 1)}{(\mathcal{C}_1^2 + r^2)^2} [r(\mathcal{C}_1^4 + 3\mathcal{C}_1^2r^2 + 2r^4)\mathcal{F}'(r) - 2(\mathcal{C}_1^4 + 2\mathcal{C}_1^2r^2 + 2r^4)\mathcal{F}(r)] \\ & + \frac{1}{(\chi_3 + 2\pi)(\chi_3 + 4\pi)\mathcal{C}_3^2(\mathcal{C}_1^2 + 2r^2)^2} \left[2r(45\pi\mathcal{C}_1^6\chi_3 + 2\mathcal{C}_1^4(120\chi_6r^4\mathcal{C}_3^2\chi_3^2 \right. \\ & \times (\chi_3 + 1) + 96\pi^2\chi_6r^4\mathcal{C}_3^2 + 5\pi\chi_3(8\chi_6r^4\mathcal{C}_3^2(6\chi_3 + 7) + 15r^2 + 9\mathcal{C}_3^2)) \\ & + 4\mathcal{C}_1^2(240\chi_6r^6\mathcal{C}_3^2\chi_3^2(\chi_3 + 1) + 5\pi r^2\chi_3(24r^2 + 15\mathcal{C}_3^2 + 16(6\chi_3 + 7) \\ & \times \chi_6r^4\mathcal{C}_3^2) + 48\pi^2r^4(4\chi_6r^2\mathcal{C}_3^2 + 5)) + 64r^4\mathcal{C}_3^2(15\chi_6r^4\chi_3^2(\chi_3 + 1) + 5\pi\chi_3 \\ & \times (\chi_6r^4(6\chi_3 + 7) + 3) + 6\pi^2(2\chi_6r^4 + 5)) - 45\sqrt{2}\pi\sqrt{\mathcal{C}_1^2\chi_3}(\mathcal{C}_1^2 + 2r^2)^2 \\ & \left. \times (\mathcal{C}_1^2 + 2\mathcal{C}_3^2) \tan^{-1} \left(\frac{\sqrt{2}r}{\sqrt{\mathcal{C}_1^2}} \right) \right] - 120r(2\mathcal{F}(r) - r\mathcal{F}'(r)) = 0. \end{aligned} \quad (63)$$

The solution belonging to the above equation is

$$\mathcal{F}(r) = \frac{r^2(\mathcal{C}_1^2 + r^2)}{120\mathcal{C}_3^2(\chi_3^2 + 6\pi\chi_3 + 8\pi^2)(\chi_3\mathcal{C}_1^2 + 2\mathcal{C}_1^2 + 2\chi_3r^2 + 3r^2)} \left[(\mathcal{C}_1^2 + 2\mathcal{C}_3^2) \right]$$

$$\begin{aligned}
& \times \left\{ \frac{30\pi\chi_3}{r^2} + \frac{60\pi(3\chi_3 + 8\pi)}{\mathcal{C}_1^2 + 2r^2} - \frac{15\chi_3\sqrt{2\mathcal{C}_1^2} \tan^{-1}\left(\frac{\sqrt{2}r}{\sqrt{\mathcal{C}_1^2}}\right)}{r^3} \right\} - 16\chi_6 r^2 \\
& \times \left\{ 12\pi^2 + 15\chi_3^2(1 + \chi_3) + 5\pi\chi_3(7 + 6\chi_3) \right\} + \frac{\mathbb{C}_3 r^2 (\mathcal{C}_1^2 + r^2)}{\chi_3 \mathcal{C}_1^2 + 2\mathcal{C}_1^2 + 2\chi_3 r^2 + 3r^2}, \tag{64}
\end{aligned}$$

where \mathbb{C}_3 being an integration constant with dimension $\frac{1}{l^2}$. The transformation (18) modifies the radial coefficient in terms of the function (64) as

$$e^{\chi_2} = \chi_5^{-1} = \frac{\mathcal{C}_3^2 (\mathcal{C}_1^2 + 2r^2)}{(\mathcal{C}_1^2 + r^2)(\mathcal{C}_3^2 - r^2) + \gamma \mathcal{C}_3^2 \mathcal{F}(r) (\mathcal{C}_1^2 + 2r^2)}. \tag{65}$$

Hence, the corresponding matter determinants take the final form as

$$\begin{aligned}
\bar{\mu} = & \frac{9\mathcal{C}_1^2(3\chi_3 + 8\pi) - r^2(5\chi_3 + 12\pi)\chi_6(\mathcal{C}_1^2 + 3r^2)^2 + 6r^2(5\chi_3 + 12\pi)}{12(\chi_3 + 2\pi)(\chi_3 + 4\pi)(\mathcal{C}_1^2 + 3r^2)^2} \\
& - \frac{\gamma}{960\pi\mathcal{C}_3^2(\mathcal{C}_1^2(\chi_3 + 2) + r^2(2\chi_3 + 3))^2} \left[120\mathcal{C}_3^2\mathbb{C}_3(\mathcal{C}_1^2 r^2(7\chi_3 + 13) + 3 \right. \\
& \times \mathcal{C}_1^4(\chi_3 + 2) + 3r^4(2\chi_3 + 3)) + \frac{30\pi\mathcal{C}_1^2}{r(\chi_3 + 2\pi)(\chi_3 + 4\pi)(\mathcal{C}_1^2 + 2r^2)^2} \\
& \times \left\{ 4\mathcal{C}_1^2 r^5(\chi_3(14\chi_3 + 32\pi + 27) + 60\pi) + 8\mathcal{C}_1^4 r^3(\chi_3(7\chi_3 + 18\pi + 14) \right. \\
& + 34\pi) + 4\sqrt{2}\mathcal{C}_1^3 r^4 \chi_3(\chi_3 + 1) \tan^{-1}\left(\frac{\sqrt{2}r}{\sqrt{\mathcal{C}_1^2}}\right) + 4\sqrt{2}\mathcal{C}_1^5 r^2 \chi_3(\chi_3 + 1) \\
& \times \tan^{-1}\left(\frac{\sqrt{2}r}{\sqrt{\mathcal{C}_1^2}}\right) + 2\mathcal{C}_1^6 r(\chi_3(9\chi_3 + 24\pi + 19) + 48\pi) + \sqrt{2}(\chi_3 + 1) \\
& \times \mathcal{C}_1^7 \chi_3 \tan^{-1}\left(\frac{\sqrt{2}r}{\sqrt{\mathcal{C}_1^2}}\right) + 16r^7(\chi_3 + 2\pi)(2\chi_3 + 3) \left. \right\} + 4\mathcal{C}_3^2 \{ r(\chi_3 + 2\pi) \\
& \times (\chi_3 + 4\pi)(\mathcal{C}_1^2 + 2r^2)^2 \}^{-1} \left\{ 6\mathcal{C}_1^6 r(5\pi(\chi_3(9\chi_3 + 24\pi + 19) + 48\pi) \right. \\
& - 2r^4(11\chi_3 + 21)(5\chi_3(3\chi_3(\chi_3 + 2\pi + 1) + 7\pi) + 12\pi^2)\chi_6) + 60\sqrt{2}\pi\mathcal{C}_1^3 \\
& \times r^4 \chi_3(\chi_3 + 1) \tan^{-1}\left(\frac{\sqrt{2}r}{\sqrt{\mathcal{C}_1^2}}\right) - 20\mathcal{C}_1^8 r^3(\chi_3 + 2)(5\chi_3(3\chi_3(\chi_3 + 2\pi + 1)
\end{aligned}$$

$$\begin{aligned}
& + 7\pi) + 12\pi^2)\chi_6 + 60\sqrt{2}\pi\mathcal{C}_1^5r^2\chi_3(\chi_3 + 1) \tan^{-1}\left(\frac{\sqrt{2}r}{\sqrt{\mathcal{C}_1^2}}\right) + 4\mathcal{C}_1^2r^5(15\pi \\
& \times (\chi_3(14\chi_3 + 32\pi + 27) + 60\pi) - 4r^4(23\chi_3 + 38)(5\chi_3(3\chi_3(\chi_3 + 2\pi + 1) \\
& + 7\pi) + 12\pi^2)\chi_6) + 4\mathcal{C}_1^4r^3(30\pi(\chi_3(7\chi_3 + 18\pi + 14) + 34\pi) - r^4(82\chi_3 \\
& + 147)(5\chi_3(3\chi_3(\chi_3 + 2\pi + 1) + 7\pi) + 12\pi^2)\chi_6) + 15\sqrt{2}\pi\mathcal{C}_1^7\chi_3(\chi_3 + 1) \\
& \times \tan^{-1}\left(\frac{\sqrt{2}r}{\sqrt{\mathcal{C}_1^2}}\right) + 80r^7(2\chi_3 + 3)(3\pi(\chi_3 + 2\pi) - r^4((3\chi_3(\chi_3 + 2\pi + 1) \\
& + 7\pi)5\chi_3 + 12\pi^2)\chi_6) \left. \right\} \Bigg], \tag{66}
\end{aligned}$$

$$\begin{aligned}
\bar{P}_r = & \frac{1}{960} \left[\frac{80\{r^2(5\chi_3 + 12\pi)\chi_6(\mathcal{C}_1^2 + 3r^2)^2 + 3\chi_3(3\mathcal{C}_1^2 + 2r^2)\}}{(\chi_3 + 2\pi)(\chi_3 + 4\pi)(\mathcal{C}_1^2 + 3r^2)^2} + \gamma r^2 \{ \pi \right. \\
& \times (\mathcal{C}_1^2(\chi_3 + 2) + r^2(2\chi_3 + 3))\mathcal{C}_3^2(\chi_3 + 2\pi)(\chi_3 + 4\pi) \}^{-1}(\mathcal{C}_1^2 + r^2) \\
& \times \left(\frac{2}{\mathcal{C}_1^2 + r^2} + \frac{1}{r^2} \right) \left\{ 120\mathcal{C}_3\mathcal{C}_3^2(\chi_3 + 2\pi)(\chi_3 + 4\pi) - 15\sqrt{2}\pi r^{-3}\mathcal{C}_1\chi_3 \right. \\
& \times (\mathcal{C}_1^2 + 2\mathcal{C}_3^2) \tan^{-1}\left(\frac{\sqrt{2}r}{\sqrt{\mathcal{C}_1^2}}\right) - 16\mathcal{C}_3^2r^2(5\chi_3(3\chi_3(\chi_3 + 2\pi + 1) + 7\pi) \\
& \left. + 12\pi^2)\chi_6 + 30\pi r^{-2}(\mathcal{C}_1^2 + 2\mathcal{C}_3^2)\chi_3 + \frac{60\pi(\mathcal{C}_1^2 + 2\mathcal{C}_3^2)(3\chi_3 + 8\pi)}{\mathcal{C}_1^2 + 2r^2} \right\} \Bigg], \tag{67}
\end{aligned}$$

$$\begin{aligned}
\bar{P}_\perp = & \frac{3(\chi_3(3\mathcal{C}_1^2 + 8r^2) + 12\pi r^2) - r^2(7\chi_3 + 12\pi)\chi_6(\mathcal{C}_1^2 + 3r^2)^2}{12(\chi_3 + 2\pi)(\chi_3 + 4\pi)(\mathcal{C}_1^2 + 3r^2)^2} + \gamma r^2 \\
& \times (2\mathcal{C}_1^2 + r^2) \{ 960\pi\mathcal{C}_3^2(\chi_3 + 2\pi)(\chi_3 + 4\pi)(\mathcal{C}_1^2 + r^2)(\mathcal{C}_1^2(\chi_3 + 2) \\
& + r^2(2\chi_3 + 3)) \}^{-1} \left\{ 120\mathcal{C}_3\mathcal{C}_3^2(\chi_3 + 2\pi)(\chi_3 + 4\pi) - 15\sqrt{2}\pi r^{-3}\mathcal{C}_1\chi_3 \right. \\
& \times (\mathcal{C}_1^2 + 2\mathcal{C}_3^2) \tan^{-1}\left(\frac{\sqrt{2}r}{\sqrt{\mathcal{C}_1^2}}\right) - 16\mathcal{C}_3^2r^2(5\chi_3(3\chi_3(\chi_3 + 2\pi + 1) + 7\pi) \\
& \left. + 12\pi^2)\chi_6 + 30\pi r^{-2}(\mathcal{C}_1^2 + 2\mathcal{C}_3^2)\chi_3 + \frac{60\pi(\mathcal{C}_1^2 + 2\mathcal{C}_3^2)(3\chi_3 + 8\pi)}{\mathcal{C}_1^2 + 2r^2} \right\} \\
& + \frac{\gamma r^{-2}\mathcal{C}_3^{-2}}{960\pi(\mathcal{C}_1^2(\chi_3 + 2) + r^2(2\chi_3 + 3))^2(\chi_3 + 2\pi)(\chi_3 + 4\pi)(\mathcal{C}_1^2 + 2r^2)^2}
\end{aligned}$$

$$\begin{aligned}
& \times \left(\frac{r}{2(\mathcal{C}_1^2 + r^2)} + \frac{1}{2r} \right) \left[240\mathcal{C}_3\mathcal{C}_3^2r^3(2r^2\mathcal{C}_1^2(\chi_3 + 2) + \mathcal{C}_1^4(\chi_3 + 2) + r^4 \right. \\
& \times (2\chi_3 + 3))(\chi_3 + 2\pi)(\chi_3 + 4\pi)(\mathcal{C}_1^2 + 2r^2)^2 - 256\mathcal{C}_3^2r^{13}(2\chi_3 + 3) \\
& \times (5\chi_3(3\chi_3(\chi_3 + 2\pi + 1) + 7\pi) + 12\pi^2)\chi_6 + 120\sqrt{2}\pi\mathcal{C}_1\mathcal{C}_3^2r^8\chi_3(2\chi_3 \\
& + 3) \tan^{-1} \left(\frac{\sqrt{2}r}{\sqrt{\mathcal{C}_1^2}} \right) + 15\sqrt{2}\pi\mathcal{C}_1^7r^2\chi_3(6\mathcal{C}_3^2(3\chi_3 + 5) + 13r^2(2\chi_3 + 3)) \\
& \times \tan^{-1} \left(\frac{\sqrt{2}r}{\sqrt{\mathcal{C}_1^2}} \right) + 15\sqrt{2}\pi\mathcal{C}_1^9\chi_3(2\mathcal{C}_3^2(\chi_3 + 2) + 3r^2(3\chi_3 + 5)) \\
& \tan^{-1} \left(\frac{\sqrt{2}r}{\sqrt{\mathcal{C}_1^2}} \right) + 24\mathcal{C}_1^2\mathcal{C}_3^2r^7(-16r^4(3\chi_3 + 5)(5\chi_3(3\chi_3(\chi_3 + 2\pi + 1) \\
& + 7\pi) + 12\pi^2)\chi_6 - 5\pi\chi_3(6\chi_3 + 1) + 80\pi^2) + 60\sqrt{2}\pi\mathcal{C}_1^3r^6\chi_3(2\mathcal{C}_3^2(7\chi_3 \\
& + 10) + r^2(2\chi_3 + 3)) \tan^{-1} \left(\frac{\sqrt{2}r}{\sqrt{\mathcal{C}_1^2}} \right) + 2\mathcal{C}_1^8r(15\pi(\chi_3((5\chi_3 + 32\pi + 13) \\
& \times r^2 - 2\mathcal{C}_3^2(\chi_3 + 2)) + 64\pi r^2) - 32\mathcal{C}_3^2r^4(\chi_3 + 2)(5\chi_3(3\chi_3(\chi_3 + 2\pi + 1) \\
& + 7\pi) + 12\pi^2)\chi_6) + 30\sqrt{2}\pi\mathcal{C}_1^5r^4\chi_3(13\mathcal{C}_3^2(2\chi_3 + 3) + 2r^2(7\chi_3 + 10)) \\
& \times \tan^{-1} \left(\frac{\sqrt{2}r}{\sqrt{\mathcal{C}_1^2}} \right) + 4\mathcal{C}_1^4r^5(\mathcal{C}_3^2(15\pi(\chi_3(8\chi_3 + 64\pi + 27) + 128\pi) - 16r^4 \\
& \times (16\chi_3 + 29)(5\chi_3(3\chi_3(\chi_3 + 2\pi + 1) + 7\pi) + 12\pi^2)\chi_6) + 15\pi r^2(16\pi \\
& - \chi_3(6\chi_3 + 1))) + 2\mathcal{C}_1^6r^3(2\mathcal{C}_3^2(15\pi(\chi_3(5\chi_3 + 32\pi + 13) + 64\pi) - 8r^4 \\
& \times (13\chi_3 + 25)(5\chi_3(3\chi_3(\chi_3 + 2\pi + 1) + 7\pi) + 12\pi^2)\chi_6) + 15\pi r^2(\chi_3 \\
& \times (8\chi_3 + 64\pi + 27) + 128\pi)) - 30\pi\mathcal{C}_1^{10}r\chi_3(\chi_3 + 2) + 15\sqrt{2}\pi\mathcal{C}_1^{11}\chi_3 \\
& \left. \times (\chi_3 + 2) \tan^{-1} \left(\frac{\sqrt{2}r}{\sqrt{\mathcal{C}_1^2}} \right) \right], \tag{68}
\end{aligned}$$

and the corresponding anisotropy can be obtained by taking the difference of Eqs.(67) and (68).

6 Graphical Analysis of the Obtained Models

A numerical solution of the following first-order differential equation yields the mass of a spherical fluid configuration by

$$\frac{d\bar{m}(r)}{dr} = 4\pi r^2 \bar{\mu}, \quad (69)$$

where $\bar{\mu}$ (involving $f(\mathbb{R}, \mathbb{T})$ corrections) is presented in Eqs.(43) and (66) for the first and second models, respectively. We solve the above equation for an initial condition $\bar{m}(0) = 0$. The particles in any self-gravitating system arranged in some particular manner which helps to know the compactness ($\tau(r)$) in that body. The tightness of the particles by which they are ordered in a system can also be measured with the help of this factor. Moreover, the mass-radius ratio also helps to estimate $\tau(r)$. A feasible spherical structure must possess its maximum value by $\frac{4}{9}$ [51]. The interesting fact about a compactness factor is that the wavelength of an electromagnetic radiations emit by a celestial body necessarily affect by it. A sufficient attractive gravitational force in a compact star changes the path in which those radiations move. Based on the above discussion, we specify the redshift in the following manner

$$z(r) = \frac{1 - \sqrt{1 - 2\tau(r)}}{\sqrt{1 - 2\tau(r)}}, \quad (70)$$

whose maximum value at the spherical surface is 2 (or 5.211) for perfect [51] (or anisotropic [52]) fluids, respectively.

Certain constraints are of great importance in the field of astronomy to check the physical viability of the obtained models in any theory of gravity. These bounds also help to check whether there exists a usual matter in the interior of a compact star or not. They are termed as the energy conditions in the literature whose dissatisfaction guarantees the presence of an exotic fluid. The energy conditions are the linear combinations of different matter determinants (i.e., density and pressure) that must be fulfilled for an acceptable model. They take the form for the considered scenario as

$$\begin{aligned} \bar{\mu} + \frac{s^2}{8\pi r^4} &\geq 0, & \bar{\mu} + \bar{P}_r &\geq 0, \\ \bar{\mu} + \bar{P}_\perp + \frac{s^2}{4\pi r^4} &\geq 0, & \bar{\mu} - \bar{P}_r + \frac{s^2}{4\pi r^4} &\geq 0, \end{aligned}$$

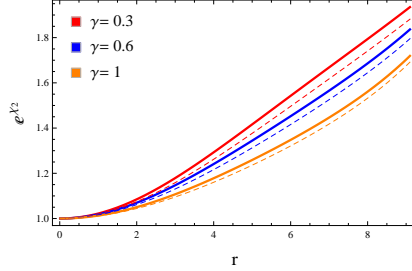


Figure 1: Deformed g_{rr} metric function (41) versus r (in km) for $\bar{\mathcal{S}} = 0.1$ (solid lines) and $\bar{\mathcal{S}} = 0.8$ (dashed lines) corresponding to $\bar{\Pi} = 0$.

$$\bar{\mu} - \bar{P}_{\perp} \geq 0, \quad \bar{\mu} + \bar{P}_r + 2\bar{P}_{\perp} + \frac{s^2}{4\pi r^4} \geq 0. \quad (71)$$

The stability plays a crucial role in the analysis of the evolution of self-gravitating models. We shall discuss this phenomenon with the help of two strategies in the following. Firstly, we define the sound speeds in radial ($V_{sr}^2 = \frac{d\bar{P}_r}{d\bar{\mu}}$) and tangential ($V_{s\perp}^2 = \frac{d\bar{P}_{\perp}}{d\bar{\mu}}$) directions. It was pointed out that the speed of sound in a medium must be less than that of light to maintain the causality, i.e., $0 < V_{sr}^2, V_{s\perp}^2 < 1$ [53]. Another criterion to do so has been suggested by Herrera [54, 55], according to which the inequality $0 < |V_{s\perp}^2 - V_{sr}^2| < 1$ should hold to get a physically stable model.

We adopt the $f(\mathbb{R}, \mathbb{T})$ model (11) to discuss the graphical interpretation of the both resulting charged solutions, their corresponding deformation functions as well as the complexity factors. For the first solution, different values of the decoupling parameter and charge along with an integration constant $\mathbb{C}_1 = -0.003$ and $\chi_3 = 0.3$ are chosen so that the corresponding physical characteristics can be explored. Figure 1 assures an acceptable (singularity free and increasing outwards) behavior of the deformed g_{rr} potential (41) for $0 < r < \mathcal{R}$. A resulting model would be found acceptable only if the governing state parameters representing interior distribution (like the energy density and pressure) are maximum (minimum) and positively finite at the center (boundary) of an astrophysical body. Figure 2 depicts such behavior for the first solution being represented by Eqs.(43)-(46). The upper left plot of the energy density shows its maximum value in the star's core. However, the increment in the decoupling parameter as well as an electric charge decreases the density of the fluid. On the other hand, the pressure in radial and transverse directions shows the opposite behavior to that of the density

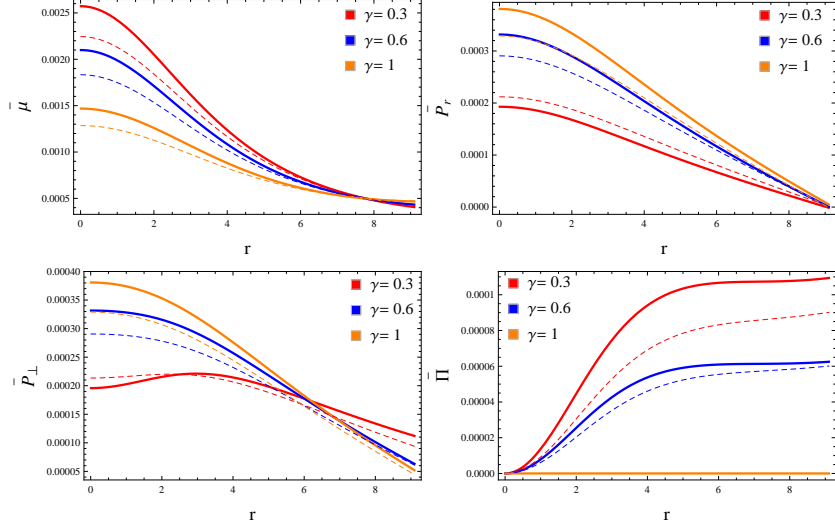


Figure 2: Matter determinants and anisotropy (in km^{-2}) versus r (in km) for $\bar{S} = 0.1$ (solid lines) and $\bar{S} = 0.8$ (dashed lines) corresponding to $\bar{\Pi} = 0$.

corresponding to the parameter γ . Additionally, the pressure components decrease with the increment in an electric charge. The star's boundary contains only the tangential pressure while the radial one disappears at that point. Figure 2 (last plot) also exhibits the plot of the anisotropic factor that vanishes only at the core for $\gamma = 0.3, 0.6$ and throughout for $\gamma = 1$. Hence, the isotropization of the developed solution is clearly observed from the graphical analysis.

Figure 3 presents the mass function of the corresponding spherical self-gravitating model. We find the charged/uncharged isotropic system to be less dense in comparison with the respective anisotropic analog. Moreover, we calculate the resulting mass at the spherical boundary in terms of mass of the sun for all parametric choices and deduced that this model fits best with the observational mass for $\gamma = 0.3$ and $\bar{S} = 0.1$, i.e., $\bar{\mathcal{M}} = 1.56M_\odot$. The other two parameters plotted in the same Figure guarantee the fulfillment of their respective criteria. The positive trend shown by the state variables (in Figure 2) allows us to plot only the dominant energy conditions such as $\bar{\mu} - \bar{P}_r + \frac{s^2}{4\pi r^4} \geq 0$ and $\bar{\mu} - \bar{P}_\perp \geq 0$. These bounds can be seen in Figure 4 from which the viability of the resulting model is revealed. Moreover, multiple strategies are used in Figure 5 to check whether our solution is

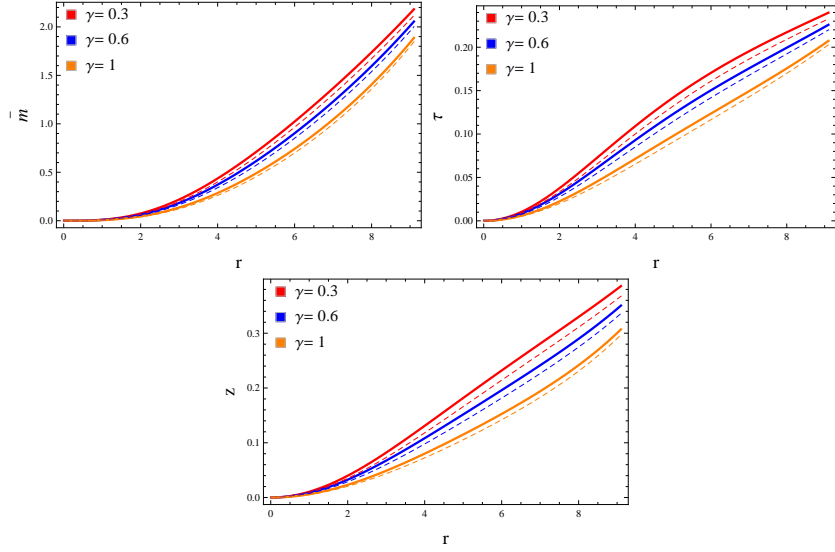


Figure 3: Mass (in km), compactness and redshift versus r (in km) for $\bar{S} = 0.1$ (solid lines) and $\bar{S} = 0.8$ (dashed lines) corresponding to $\bar{\Pi} = 0$.

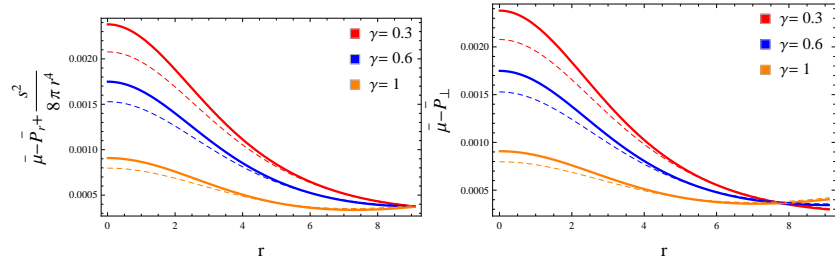


Figure 4: Dominant energy conditions (in km^{-2}) versus r (in km) for $\bar{S} = 0.1$ (solid lines) and $\bar{S} = 0.8$ (dashed lines) corresponding to $\bar{\Pi} = 0$.

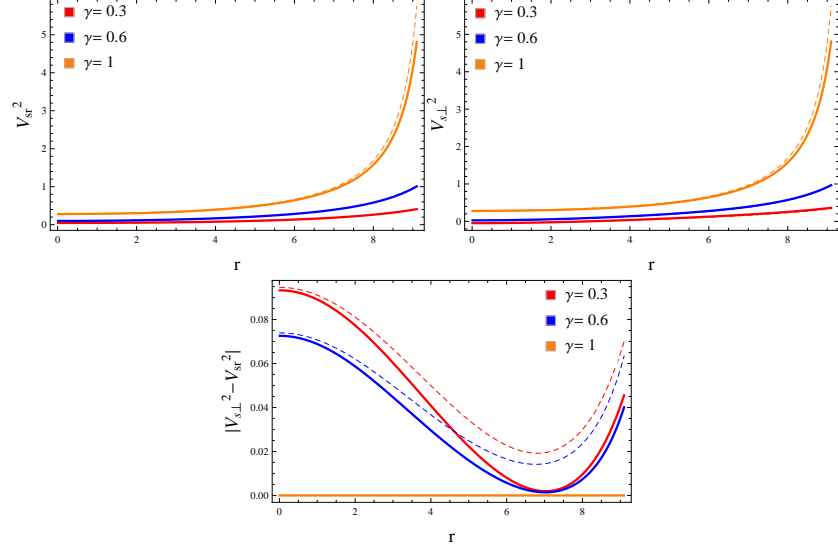


Figure 5: Radial/tangential sound speeds and cracking criteria versus r (in km) for $\bar{S} = 0.1$ (solid lines) and $\bar{S} = 0.8$ (dashed lines) corresponding to $\bar{\Pi} = 0$.

stable or unstable. The upper two plots provide that $\gamma = 0.6$ (with $\bar{S} = 0.1$ and 0.8) is the only parametric value for which both sound speeds show stable behavior. Contrariwise, we get the stable model for every choice of γ through the cracking criteria (lower plot). Figure 6 exhibits that the modified scalar factors (51) and (62) decrease and increase, respectively, by increasing the decoupling parameter. However, both factors are in an inverse relation with an electric charge. Further, we compare the behavior of this factor with that of $\mathbb{G}\mathbb{R}$ and deduce that the complexity reduces in the former case.

The physical properties of the second solution corresponding to $\bar{Y}_{TF} = 0$ is now explored for the same values of γ and χ_3 along with $\mathbb{C}_3 = -0.001$. Figure 7 shows that the deformed g_{rr} component possesses singularity-free and increasing nature. The plots of the matter triplet (provided in Eqs.(66)-(68)) and anisotropic factor are demonstrated in Figure 8. They own the same trend as already observed for the first solution. The last plot exhibits that the core (boundary) of a compact star contains no (maximum) anisotropy for all chosen parametric values. However, the increment in charge results in less anisotropy. Figure 9 indicates that the greater the value of γ and charge, the less the mass of a compact star is. Further, the required criteria

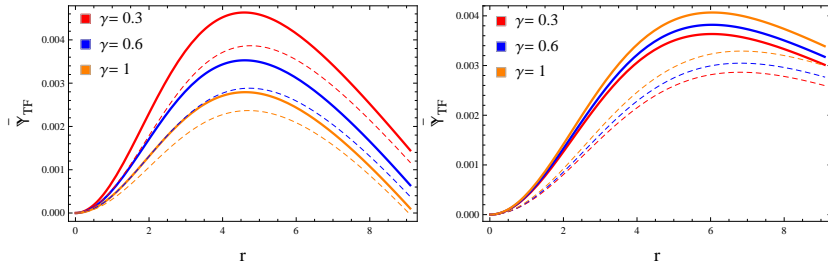


Figure 6: Complexity factors (51) and (62) (in km^{-2}) versus r (in km) for $\bar{\mathcal{S}} = 0.1$ (solid lines) and $\bar{\mathcal{S}} = 0.8$ (dashed lines).

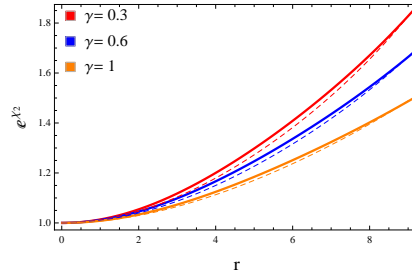


Figure 7: Deformed g_{rr} metric function (65) versus r (in km) for $\bar{\mathcal{S}} = 0.1$ (solid lines) and $\bar{\mathcal{S}} = 0.8$ (dashed lines) corresponding to $\bar{\mathcal{Y}}_{TF} = 0$.

for the redshift and compactness parameters is fulfilled, as can be seen from the same Figure. The plots in Figure 10 guarantee that the corresponding solution is viable. Figure 11 reveals that our resulting model (66)-(68) is stable for all parametric choices except $\gamma = 1$ (upper left plot).

7 Conclusions

This paper explores the existence of self-gravitating spherical anisotropic charged models by extending the original solutions to an additional matter field by using the strategy of gravitational decoupling in $f(\mathbb{R}, \mathbb{T}) = \mathbb{R} + 2\chi_3\mathbb{T}$ theory. We initially added the Lagrangian densities of the electromagnetic field and extra source in the action and formulated the corresponding field equations. We then separated the effects of the seed and extra matter sources by dividing the field equations into two individual sets by employing the MGD scheme. The influence of the charge has only been observed in the

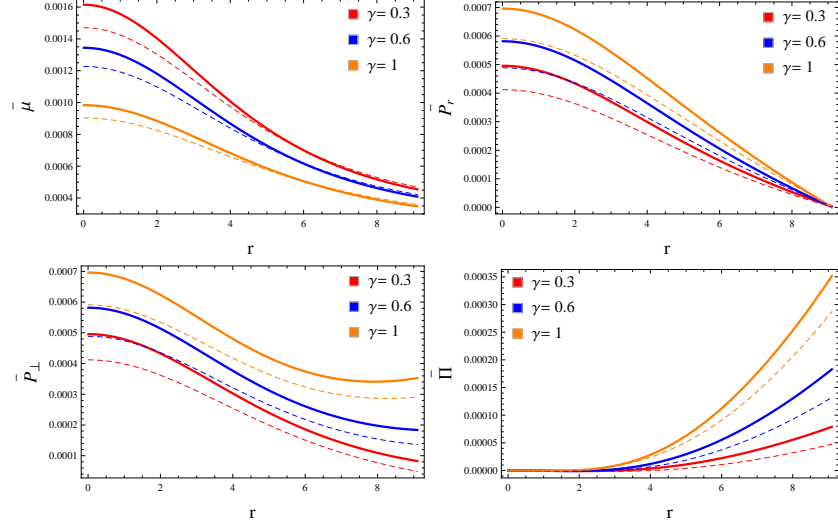


Figure 8: Matter determinants and anisotropy (in km^{-2}) versus r (in km) for $\bar{\mathcal{S}} = 0.1$ (solid lines) and $\bar{\mathcal{S}} = 0.8$ (dashed lines) corresponding to $\bar{\mathbb{Y}}_{TF} = 0$.

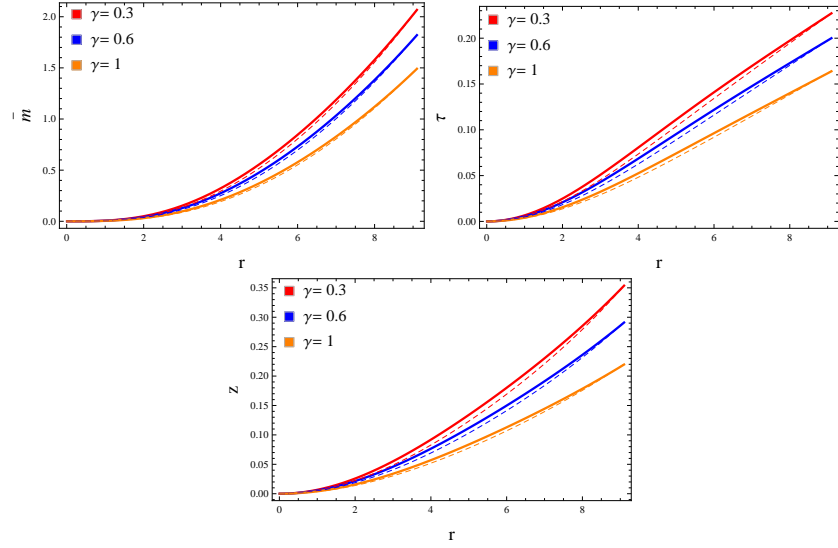


Figure 9: Mass (in km), compactness and redshift versus r (in km) for $\bar{\mathcal{S}} = 0.1$ (solid lines) and $\bar{\mathcal{S}} = 0.8$ (dashed lines) corresponding to $\bar{\mathbb{Y}}_{TF} = 0$.

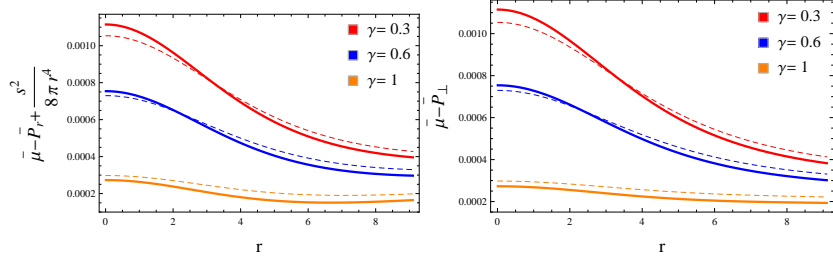


Figure 10: Dominant energy conditions (in km^{-2}) versus r (in km) for $\bar{S} = 0.1$ (solid lines) and $\bar{S} = 0.8$ (dashed lines) corresponding to $\bar{Y}_{TF} = 0$.

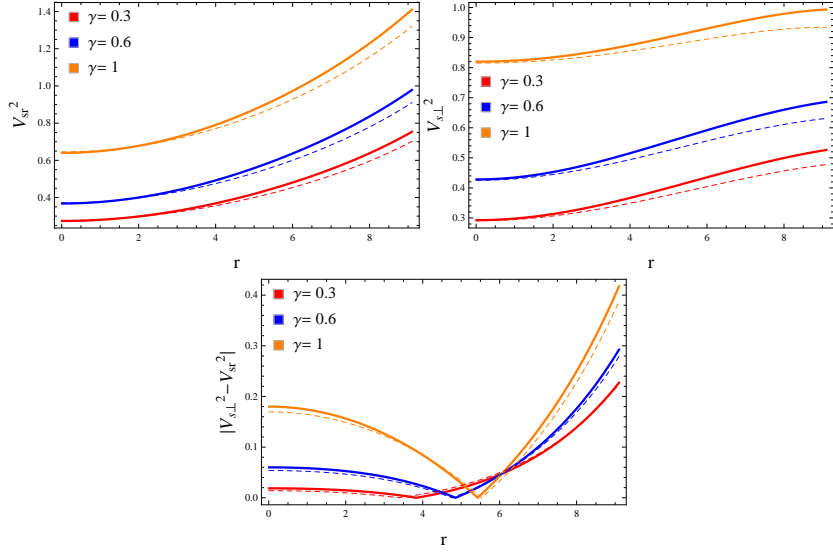


Figure 11: Radial/tangential sound speeds and cracking criteria versus r (in km) for $\bar{S} = 0.1$ (solid lines) and $\bar{S} = 0.8$ (dashed lines) corresponding to $\bar{Y}_{TF} = 0$.

field equations representing the original matter distribution. Two different solutions to this set were obtained by taking the following ansatz

$$\chi_1(r) = \ln \left\{ \mathcal{C}_2^2 \left(1 + \frac{r^2}{\mathcal{C}_1^2} \right) \right\}, \quad \chi_5(r) = e^{-\chi_2(r)} = \frac{\mathcal{C}_1^2 + r^2}{\mathcal{C}_1^2 + 3r^2},$$

and Tolman IV spacetime, respectively. These metric potentials contain a triplet $(\mathcal{C}_1, \mathcal{C}_2, \mathcal{C}_3)$ as unknown quantities whose values have been calculated through continuity of the metric potentials at the spherical boundary. The other set (25)-(27) encoding the effect of the additional source was then solved by employing some constraints on $\mathfrak{C}_{\beta\alpha}$. We have constructed an isotropic model from being anisotropic for a particular value, i.e., $\gamma = 1$, leading to the first solution. Further, the second model was developed by taking into consideration that the resultant complexity factor corresponding to both matter sectors becomes null.

Different values of the decoupling parameter along with fixed values of the coupling as well as integration constants have been chosen to graphically analyze the developed solutions so that we can check how γ influences these extended models. The matter determinants for both solutions (presented in (43)-(45) and (66)-(68)), their corresponding anisotropic factors, redshift, compactness and the energy conditions have shown an acceptable behavior. It was also observed that the first resulting model corresponding to $\bar{\Pi} = 0$ possesses a dense interior for every value of γ in comparison with the second solution. Further, the radial metric components (41) and (65) have been deformed and plotted which exhibit positive and increasing behavior throughout (Figures 1 and 7). We have employed the causality and cracking criteria to analyze whether the modified models show stable behavior for all choices of the decoupling parameter and charge or not. We have observed that the first model is stable only for $\gamma = 0.6$ through the causality conditions, and thus compatible with the uncharged $f(\mathbb{R}, \mathbb{T})$ framework [9] as well as Brans-Dicke theory only for this value [47]. However, the cracking criterion provides both stable solutions. Eventually, all these results can be reduced to \mathbb{GR} for $\chi_3 = 0$.

Data Availability Statement: No Data associated in the manuscript.

Conflict of Interest Statement: The authors declare that there is no conflict of interest.

References

- [1] Capozziello, S. et al.: *Class. Quantum Grav.* **25**(2008) 085004; Nojiri, S. et al.: *Phys. Lett. B* **681**(2009)74.
- [2] de Felice, A. and Tsujikawa, S.: *Living Rev. Relativ.* **13**(2010)3; Nojiri, S. and Odintsov, S.D.: *Phys. Rep.* **505**(2011)59.
- [3] Sharif, M. and Kausar, H.R.: *J. Cosmol. Astropart. Phys.* **07**(2011)022.
- [4] Astashenok, A.V., Capozziello, S. and Odintsov, S.D.: *J. Cosmol. Astropart. Phys.* **01**(2015)001; *Phys. Lett. B* **742**(2015)160.
- [5] Bertolami, O. et al.: *Phys. Rev. D* **75**(2007)104016.
- [6] Harko, T. et al.: *Phys. Rev. D* **84**(2011)024020.
- [7] Houndjo, M.J.S.: *Int. J. Mod. Phys. D* **21**(2012)1250003.
- [8] Das, A. et al.: *Phys. Rev. D* **95**(2017)124011.
- [9] Sharif, M. and Naseer, T.: *Eur. Phys. J. Plus* **137**(2022)1304.
- [10] Azmat, H. and Zubair M.: *Eur. Phys. J. Plus* **136**(2018)112.; Rej, P., Bhar, Piyali. and Govender, M.: *Eur. Phys. J. C* **81**(2021)316; Zubair, M. et al.: *New Astron.* **88**(2021)101610.
- [11] Shamir, M.F., Asghar, Z. and Malik, A.: *Fortschr. Phys.* **70**(2022)2200134; Malik, A., Yousaf, Z., Jan, M., Shahzad, M.R. and Akram, Z.: *Int. J. Geom. Methods Mod.* **20**(2023)2350061.
- [12] Koussour, M. and Bennai, M.: *Int. J. Geom. Methods Mod.* **19**(2022)2250038; Myrzakulov, N., Koussour, M., Alfedeel, A.H.A. and Hassan, E.I.: *Chin. Phys. C* (2023) 10.1088/1674-1137/acf2fa.
- [13] Bora, J. and Goswami, U.D.: *Phys. Dark Universe* **38**(2022)101132; Pretel, J.M.Z.: *Mod. Phys. Lett. A* **37**(2022)2250188.
- [14] Pappas, T.D., Posada, C. and Stuchlík, Z.: *Phys. Rev. D* **106**(2022)124014; Nashed, G.G.L.: *Astrophys. J.* **950**(2023)129.

- [15] Malik, A., Asghar, Z. and Shamir, M.F.: *New Astron.* **104**(2023)102071; Asghar, Z., Shamir, M.F., Usman, A. and Malik, A.: *Chin. J. Phys.* **83**(2023)427.
- [16] Harko, T. et al.: *Phys. Rev. D* **84**(2011)024020.
- [17] Carvalho, G.A. et al.: *Eur. Phys. J. C* **77**(2017)871.
- [18] Ordines, T.M. and Carlson, E.D.: *Phys. Rev. D* **99**(2019)104052.
- [19] Carvalho, G.A. et al.: *Eur. Phys. J. C* **77**(2017)871.
- [20] Velten, H. and Caramês, T.R.P.: *Phys. Rev. D* **95**(2017)123536.
- [21] Bhattacharjee, S. and Sahoo, P.K.: *Grav. Cosmol.* **26**(2020)281.
- [22] Ashmita, Sarkar, P. and Das, P.K.: *Int. J. Mod. Phys. D* **31**(2022)2250120.
- [23] Kaur, S., Maurya, S.K., Shukla, S. and Nag, R.: *Chin. J. Phys.* **77**(2022)2854.
- [24] Ovalle, J.: *Mod. Phys. Lett. A* **23**(2008)3247.
- [25] Ovalle, J. and Linares, F.: *Phys. Rev. D* **88**(2013)104026.
- [26] Casadio, R., Ovalle, J. and Da Rocha, R.: *Class. Quantum Grav.* **32**(2015)215020.
- [27] Ovalle, J. et al.: *Eur. Phys. J. C* **78**(2018)960.
- [28] Sharif, M. and Sadiq, S.: *Eur. Phys. J. C* **78**(2018)410.
- [29] Gabbanelli, L., Rincón, Á. and Rubio, C.: *Eur. Phys. J. C* **78**(2018)370.
- [30] Estrada, M. and Tello-Ortiz, F.: *Eur. Phys. J. Plus* **133**(2018)453.
- [31] Hensh, S. and Stuchlík, Z.: *Eur. Phys. J. C* **79**(2019)834.
- [32] Sharif, M. and Majid, A.: *Chin. J. Phys.* **68**(2020)406.
- [33] Sharif, M. and Naseer, T.: *Phys. Scr.* **97**(2022)055004; *Int. J. Mod. Phys. D* **31**(2022)2240017; *Pramana* **96**(2022)119.

- [34] Bekenstein, J.D.: Phys. Rev. D **4**(1971)2185.
- [35] Esculpi, M. and Aloma, E.: Eur. Phys. J. C **67**(2010)521.
- [36] de Felice, F., Yu, Y.Q. and Fang, J.: Mon. Not. R. Astron. Soc. **277**(1995)L17.
- [37] de Felice, F., Liu, S.M. and Yu, Y.Q.: Class. Quantum Gravit. **16**(1999)2669.
- [38] Pretel, J.M.Z., Tangphati, T., Banerjee, A. and Pradhan, A.: Chin. Phys. C **46**(2022)115103.
- [39] Sharif, M. and Naseer, T.: Chin. J. Phys. **73**(2021)179; *ibid.* **81**(2023)37; *ibid.* **85**(2023)41; Phys. Scr. **97**(2022)125016; Indian J. Phys. **96**(2022)4373; Fortschr. Phys. **71**(2023)2200147.
- [40] Herrera, L.: Phys. Rev. D **97**(2018)044010.
- [41] Herrera, L., Di Prisco, A. and Ospino, J.: Phys. Rev. D **98**(2018)104059.
- [42] Yousaf, Z., Bhatti, M.Z. and Naseer, T.: Eur. Phys. J. Plus **135**(2020)353; Phys. Dark Universe **28**(2020)100535; Int. J. Mod. Phys. D **29**(2020)2050061; Ann. Phys. **420**(2020)168267.
- [43] Yousaf, Z. et al.: Phys. Dark Universe **29**(2020)100581; Yousaf, Z. et al.: Mon. Not. R. Astron. Soc. **495**(2020)4334; Sharif, M. and Naseer, T.: Chin. J. Phys. **77**(2022)2655; Eur. Phys. J. Plus **137**(2022)947.
- [44] Carrasco-Hidalgo, M. and Contreras, E.: Eur. Phys. J. C **81**(2021)757; Andrade, J. and Contreras, E.: Eur. Phys. J. C **81**(2021)889; Arias, C. et al.: Ann. Phys. **436**(2022)168671; Sharif, M. and Naseer, T.: Ann. Phys. **453**(2023)169311; Phys. Dark Universe **42**(2023)101324.
- [45] Casadio, R. et al.: Eur. Phys. J. C **79**(2019)826.
- [46] Maurya, S.K. and Nag, R.: Eur. Phys. J. C **82**(2022)48; Maurya, S.K. et al.: Eur. Phys. J. C **82**(2022)100.
- [47] Sharif, M. and Majid, A.: Eur. Phys. J. Plus **137**(2022)114.
- [48] Sharif, M. and Naseer, T.: Class. Quantum Gravit. **40**(2023)035009; Naseer, T. and Sharif, M.: Fortschr. Phys. **71**(2023)2300004.

- [49] Einstein, A.: Ann. Math. **40**(1939)922.
- [50] Güver, T., Wroblewski, P., Camarota, L. and Özel, F.: Astrophys. J. **719**(2010)1807.
- [51] Buchdahl, H.A.: Phys. Rev. **116**(1959)1027.
- [52] Ivanov, B.V.: Phys. Rev. D **65**(2002)104011.
- [53] Abreu, H., Hernandez, H. and Nunez, L.A.: Class. Quantum Gravit. **24**(2007)4631.
- [54] Herrera, L.: Phys. Lett. A **165**(1992)206; Phys. Rev. D **101**(2020)104024.
- [55] Malik, A., Shafaq, A., Naz, T. and Al-khaldi, A.H.: Eur. Phys. J. C **83**(2023)765.